

Use of Single-Metal Fragments for Cluster Building Synthesis, Structure, and Bonding of Heterometallaboranes

Bijan Mondal, Ranjit Bag, Thierry Roisnel, Sundargopal Ghosh

► To cite this version:

Bijan Mondal, Ranjit Bag, Thierry Roisnel, Sundargopal Ghosh. Use of Single-Metal Fragments for Cluster Building Synthesis, Structure, and Bonding of Heterometallaboranes. Inorganic Chemistry, American Chemical Society, 2019, 58 (4), pp.2744-2754. 10.1021/acs.inorgchem.8b03329 . hal-02050272

HAL Id: hal-02050272

<https://hal-univ-rennes1.archives-ouvertes.fr/hal-02050272>

Submitted on 22 Mar 2019

HAL is a multi-disciplinary open access archive for the deposit and dissemination of scientific research documents, whether they are published or not. The documents may come from teaching and research institutions in France or abroad, or from public or private research centers.

L'archive ouverte pluridisciplinaire **HAL**, est destinée au dépôt et à la diffusion de documents scientifiques de niveau recherche, publiés ou non, émanant des établissements d'enseignement et de recherche français ou étrangers, des laboratoires publics ou privés.

Use of Single Metal Fragments for Cluster Building: Synthesis, Structure and Bonding of Heterometalla- boranes

Bijan Mondal[†], Ranjit Bag[†], Thierry Roisnel[‡] and Sundargopal Ghosh^{†}*

[†]Department of Chemistry, Indian Institute of Technology Madras, Chennai 600 036, India.

[‡]Institut des Sciences Chimiques de Rennes, UMR 6226 CNRS-Université de Rennes 1, F-35042
Rennes Cedex, France.

Fax: (+91) 44 2257 4202; Tel: (+91) 44 2257 4230; E-mail: sghosh@iitm.ac.in.

Keywords: metallaborane, diborane, cluster, tungsten and molybdenum

ABSTRACT

Synergic property of the CO ligand in general can stabilize metal complexes at lower oxidation states. Utilizing this feature of CO ligand, we have recently isolated and structurally characterized a highly fluxional molybdenum complex $[\{\text{Cp}^*\text{Mo}(\text{CO})_2\}_2\{\mu\text{-}\eta^2\text{:}\eta^2\text{-B}_2\text{H}_4\}]$ ($\text{Cp}^* = \eta^5\text{-C}_5\text{Me}_5$) (**2**) comprising diborane(4) ligand. Compound **2** represents a rare class of bimetallic diborane(4) complex corresponding to a singly bridged *Cs* structure. In an attempt to isolate the tungsten analogue of **2**, $[\{\text{Cp}^*\text{W}(\text{CO})_2\}_2\{\mu\text{-}\eta^2\text{:}\eta^2\text{-B}_2\text{H}_4\}]$, we have isolated an rare vertex-fused cluster $[(\text{Cp}^*\text{W})_3\text{WB}_9\text{H}_{18}]$ (**5**). Having a structural likeness with dimolybdenum alkyne complex $[\{\text{CpMo}(\text{CO})_2\}_2\text{C}_2\text{H}_2]$, we have further explored the chemistry of **2** with CO gas that yielded homoleptic tri-molybdenum complex, $[(\text{Cp}^*\text{Mo})_3(\mu\text{-H})_2(\mu_3\text{-H})(\mu\text{-CO})_2\text{B}_4\text{H}_4]$ (**4**). In an attempt to replace the 16 electron $\{\text{Cp}^*\text{MoH}(\text{CO})_2\}$ moiety in **4** with isolobal fragment $\{\text{W}(\text{CO})_5\}$, we treated the intermediate, obtained from the reaction of Cp^*MoCl_4 and LiBH_4 , with mono metal carbonyl fragment $\{\text{W}(\text{CO})_5\text{.thf}\}$. The reaction indeed yielded two bimetallic clusters $[(\text{Cp}^*\text{Mo})_2\text{B}_4\text{H}_8\text{W}(\text{CO})_4]$, **7** and $[(\text{Cp}^*\text{Mo})_2\text{B}_4\text{H}_6\text{W}(\text{CO})_5]$, **8** that seem to have generated by the replacement of one $\{\text{BH}\}$ or $\{\text{BH}_3\}$ vertex from $[(\text{Cp}^*\text{Mo})_2\text{B}_5\text{H}_9]$ respectively. All of the compounds have been characterized by various spectroscopic analyses and single crystal X-ray diffraction studies. Electron counting rules and molecular orbital analyses provided further insight into the electronic structure of all these molecules.

INTRODUCTION

Boron hydrides i.e., boranes are an exceptionally diverse class¹, which are of vast importance to many areas of chemistry, both from fundamental and application standpoint.²⁻⁴ Several research groups are actively involved on this, especially diboranes and its derivatives, primarily due to its mimic of alkane counterparts.⁵ The results not only enhance our understanding of chemical

bonding⁶⁻⁷ of B_nH_{n+2} ($n = 0, 2, 4$) but also reveal their applications into homogeneous catalysis.⁸⁻⁹ The diboration reaction introduce boryl groups across the unsaturated organic species which offers valued synthetic routes.¹⁰⁻¹¹ As a result, the diboration reaction turn out to be the most-used organometallic reaction in organic synthesis of bimetallic-diborane(4).¹²

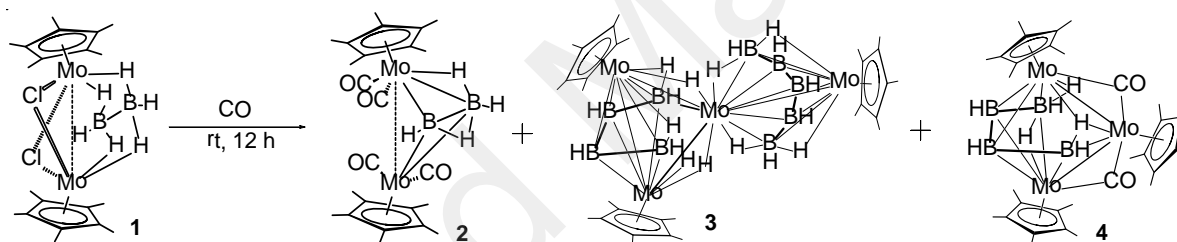
Diborane(4) compounds have been utilized as relevant starting materials to generate electron precise metal–boron bonds.¹³ For example, borylene species of the type $[\{LMn(CO)_2\}_2BR]$ ($L = \eta^5-C_5H_5$ or $\eta^5-C_5Me_5$; $R = tBu$ or NMe_2) have been synthesised from diborane(4) reagents.¹⁴ Hydrogen substituted diborane compounds, particularly, bi- or tri-metallic diborane(4) compounds, are generally very rare.¹⁵ The derivatives of B_2H_6 as well as unsubstituted B_2H_6 are found to be stabilized by the metal fragments.¹⁶⁻¹⁷ Our recent findings of bimetallic diborane(4), $[\{Cp^*Mo(CO)_2\}_2\{\mu-\eta^2:\eta^2-B_2H_4\}]$ (**2**) and diborene(2) species, $[\{Cp^*Mo(CO)_2\}_2B_2H_2W(CO)_4]$ ¹⁸ led us to explore the chemistry of **2** further, not only to increase the library but also to have substituted products within the realm of transition-metal borane chemistry.

The progress of metallaborane chemistry expanded significantly with the advancement of generalized synthetic route of group 4-9 metallaboranes.¹⁹⁻²⁰ The electronic contributions of both metal and boranes in polyhedral metallaborane clusters are expressed differently than the individuals.²¹ As a result, this makes the metallaborane chemistry more versatile and it continues to surprise with the various structural types and unusual reactivities.²² Understanding the structures of such clusters required the early development of theories on chemical bonding, e.g. Wade–Mingos or Jemmis rules for electron counting.^{23,24} Herein, in this article, we report the syntheses and structural characterizations of various metallaborane clusters using CO ligands or mono metal carbonyl fragments, $[M'(CO)_5.thf]$, ($M' = Mo$ and W). In addition, we have

performed the theoretical calculations on the ground of density functional theory (DFT) to provide further insight into their bonding and electronic structures.

RESULTS AND DISCUSSION

The metallaborane clusters of early transition metals typically yielded uncommon problems that challenged the cluster electron counting rules.²⁵ Therefore, as a part of our ongoing research on cluster growth chemistry, we intended to explore the metallaboranes of group-6 transition metals.^{18,26} As a result, we treated $[(\text{Cp}^*\text{Mo})_2(\mu\text{-Cl})_2\text{B}_2\text{H}_6]$ ²⁷ with CO, which resulted in the formation of compounds **2**, **3**²⁸ and **4** (Scheme 1). A preliminary result of diborane(4) complex **2** has recently been reported.¹⁸ The detailed spectral and structural characterization of **2** and **4** is discussed below.



Scheme 1. Synthesis of molybdaborane clusters, **2-4**.

$[(\text{Cp}^*\text{Mo}(\text{CO})_2)_2\{\mu\text{-}\eta^2\text{:}\eta^2\text{-B}_2\text{H}_4\}]$ (2**):** Reaction of $[(\text{Cp}^*\text{Mo})_2(\mu\text{-Cl})_2\text{B}_2\text{H}_6]$ ²⁷ (**1**) at ambient temperature with CO gas produces **2** that has been characterized by ¹¹B, ¹H and ¹³C NMR, and IR. The mass spectrum and IR data of **2** suggests that it is a derivative of **1**. Although, the room temperature ¹¹B NMR was uninformative, at -40 °C it showed two broad resonances appeared at $\delta = 27.3$ and -31.1 ppm, whereas the ¹H NMR showed three broad signals at $\delta = -11.3$, -0.86 and 3.28 ppm along with the signal due to Cp* ligands.

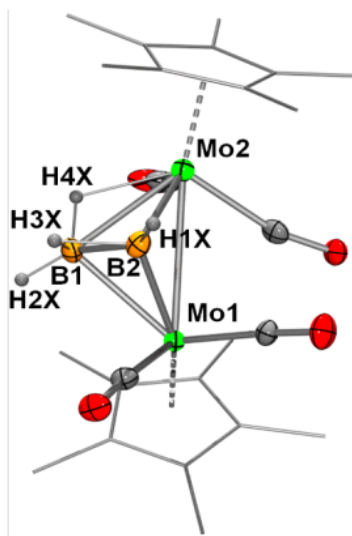


Figure 1. Molecular structure of **2** (hydrogen atoms on the Cp* ligands are omitted for clarity).

Selected bond lengths (Å) and angles (deg): B1-B2 1.700(12), B1-Mo1 2.348(9), B1-Mo2 2.420(9), B2-Mo1 2.222(8), B2-Mo2 2.366(8), Mo1-Mo2 3.0617(8), B1-H2X 1.12(10), B1-H4X 1.13(7), B1-H3X 1.09(9), B2-H1X 1.25(11), B2-H3X 1.46(9), B2-B1-Mo2 67.5(4), Mo1-B1-Mo2 79.9(3), B2-B1-H2X 139(5), Mo1-B1-H4X 115(4), Mo2-B1-H4X 47(4), H2X-B1-H4X 109(6), B2-B1-H3X 58(5), Mo1-B1-H3X 114(5), Mo2-B1-H3X 104(5), B1-B2-Mo1 72.2(4), B1-B2-Mo2 70.9(4), Mo1-B2-Mo2 83.7(3), B1-B2-H1X 155(5), Mo1-B2-H1X 128(5), Mo2-B2-H1X 121(5), Mo1-B2-H3X 105(4), Mo2-B2-H3X 95(4), B2-Mo1-B1 43.6(3), B1-Mo1-Mo2 51.1(2), B2-Mo2-Mo1 46.1(2), B1-Mo2-Mo1 49.0(2).

In order to determine the solid-state structure of **2**, the X-ray structure analysis was undertaken.

The solid-state X-ray structure (Figure 1) can be seen as $[\{\text{Cp}^*\text{Mo}(\text{CO})_2\}_2\{\mu\text{-}\eta^2\text{:}\eta^2\text{-B}_2\text{H}_4\}]$. Most noteworthy feature of **2** is the presence of a $[\text{B}_2\text{H}_4]$ moiety that is linked between two $[\text{Cp}^*\text{Mo}(\text{CO})_2]$ moieties such that the B-B bond positions perpendicular to the Mo-Mo bond. The B-B bond distance of 1.700(12) Å in **2** is significantly shorter as compared to the base stabilized diborane(4) complexes, for example, $[(\text{PMe}_3)_2\text{B}_2\text{H}_4\text{ZnCl}_2]$ (1.814(6) Å), $[(\text{PMe}_3)_2\text{B}_2\text{H}_4\text{Cr}(\text{CO})_4]$

(1.748(11) Å) and $[(\text{PMe}_3)_2\text{B}_2\text{H}_4\text{W}(\text{CO})_4]$ (1.74(41) Å).²⁹ The Mo–Mo bond distance of 3.0617(8) Å is consistent with single bond order which is comparable to those of $[\{\text{CpMo}(\text{CO})_2\}_2\{\mu\text{-}\eta^2\text{:}\eta^2\text{-C}_2\text{R}_2\}]$ (R = H/Et/Ph) (avg. 2.971(1) Å) and $[\{\text{CpMo}(\text{CO})_2\}_2\{\mu\text{-}\eta^2\text{:}\eta^2\text{-P}_2\}]$ (3.022(1) Å).³⁰ Among the different isomers of diborane(4), the singly bridged isomer with C_s symmetry is very rare and beside **2** the only such example hypothesised is $[\text{Co}_2(\text{CO})_6\text{B}_2\text{H}_4]$.³¹

Although the Cp–Mo–Mo–Cp axis in $[\{\text{CpMo}(\text{CO})_2\}_2]$ is nearly linear, the structures of both $[\{\text{CpMo}(\text{CO})_2\}_2\{\mu\text{-}\eta^2\text{:}\eta^2\text{-C}_2\text{H}_2\}]$ and **2** show distinct Mo–Mo–(Cp/Cp*) angles (Chart 1). The dihedral angle of Cp/Cp*–M–M–Cp/Cp* (147.6° vs 160.3° , see Chart 1) is related to the Cp/Cp*–M–M angle. The longer distance of B–B in comparison to that of C–C would require a more diffuse orbitals on the Cp*–M–M–Cp* in **2**. This can be achieved by bending the Cp*s farther away from the Mo–Mo axis, i.e. Cp*–M–M angle has to decrease. However, this decrease brings the two Cp*s together. The molecule reduces the Cp*---Cp* non-bonding interactions by increasing the Cp*–M–M–Cp* dihedral angle. The opening of this angle and the positioning of the carbonyls and Cp* rings over Mo–Mo bond results from the longer B–B distance (in relation to C–C) that requires a rehybridization at the metal centre for better Mo–B bonding.

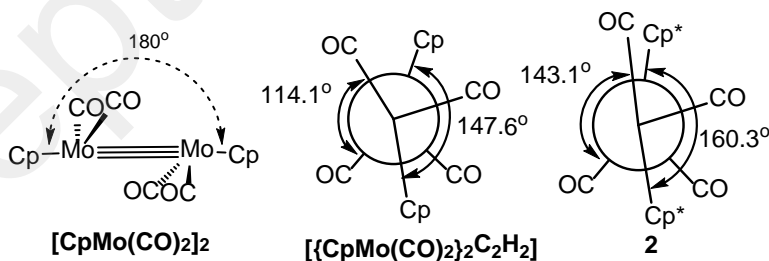


Chart 1. Schematic representation of the dihedral angles of Cp'...Mo–M...Cp' in $[\text{CpMo}(\text{CO})_2]_2$, $[\{\text{CpMo}(\text{CO})_2\}_2\text{C}_2\text{H}_2]$ and **2** (Cp' = Cp or Cp*).

Electron counting rules along with isolobal analogy suggest a close resemblance of **2**³² with $[\{\text{CpMo}(\text{CO})_2\}_2\{\mu\text{-}\eta^2\text{:}\eta^2\text{-C}_2\text{H}_2\}]$. Thus, compound **2** is a true mimic of Cotton's dimolybdenum alkyne complexes, $[\{\text{CpMo}(\text{CO})_2\}_2\{\mu\text{-}\eta^2\text{:}\eta^2\text{-C}_2\text{R}_2\}]$ (R = H/Et/Ph).^{30a} This further reveals that the $[\text{B}_2\text{H}_4]$ fragment apparently binds with the fragment $[\text{Cp}^*\text{Mo}(\text{CO})_2]_2$ (16 electron at each metal center) through four-electrons so that each Mo atom attain the 18 electron count, which is virtually similar to the bonding of $\text{RC}\equiv\text{CR}$ in $[\{\text{CpMo}(\text{CO})_2\}_2\{\mu\text{-}\eta^2\text{:}\eta^2\text{-C}_2\text{R}_2\}]$. On the other hand, adding 6 skeletal electron fragment B_2H_4 (2 BH + 2 H) to two $\{\text{CpMo}(\text{CO})_2\}$ moieties (6 skeletal electron) makes a total of 12 skeletal electrons or 6 skeletal electron pairs (seps).^{23,33} This leads to a *nido* geometry and makes compound **2** isoelectronic to $[\{\text{CpMo}(\text{CO})_2\}_2\{\mu\text{-}\eta^2\text{:}\eta^2\text{-C}_2\text{R}_2\}]$.

Homoleptic cluster, $[(\text{Cp}^*\text{Mo})_3(\mu\text{-H})_2(\mu_3\text{-H})(\mu\text{-CO})_2\text{B}_4\text{H}_4]$ (4**):** Compound **4** was isolated as a brown solid in 10% yield. The mass spectrum of **4** showed a molecular ion peak at m/z 807. The IR spectra showed strong absorption bands at 1787 and 1729 cm^{-1} corresponding to bridging CO ligands. The ^1H NMR displayed two signals at $\delta = 1.95$ and 1.91 ppm in 1:2 ratio that rationalizes the presence of two different types of Cp^* ligands. This implies two chemically dissimilar Mo environments. The presence of Cp^* and CO ligands have also been supported by ^{13}C NMR. In addition, the ^1H NMR shows three resonances in the upfield region at $\delta = -13.17$, -9.35 and -8.85 in 1:1:1 ratios, which may be due to the presence of bridged Mo-H-Mo and Mo-H-B protons. The $^{11}\text{B}\{^1\text{H}\}$ NMR spectrum shows four resonances at $\delta = 88.3$, 83.2, 46.3 and 23.5 ppm in 1:1:1:1 ratio, which demonstrates the presence of four dissimilar boron atoms in **4**. However, identity of the molecule was unambiguous and definitive structural characterization was determined by X-ray diffraction analysis on a suitable crystal obtained from a solution of compound **4** in hexane- CH_2Cl_2 solvent mixture at -10°C .

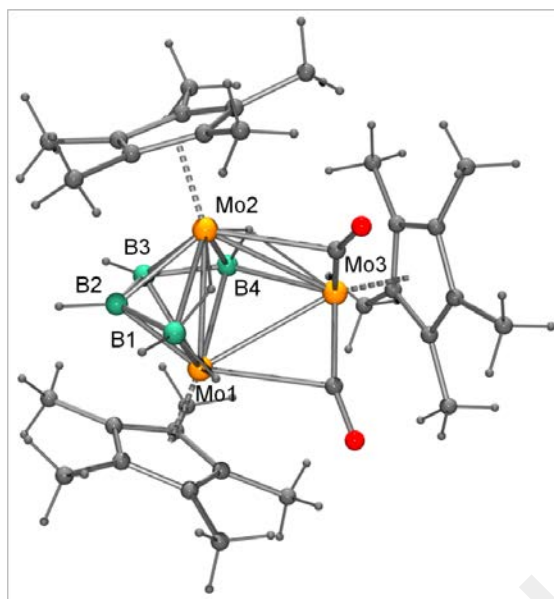


Figure 2. Molecular structure and labeling diagram for **4**. Selected bond lengths (Å) and bond angles (°): Mo1-Mo2 2.8338(5), Mo2-Mo3 2.9843(5), B1-B2 1.731(8), B2-B3 1.713(8), B3-B4 1.708(7), B1-Mo1 2.305(6), B1-Mo2 2.307(6), B2-Mo2 2.180(5), B2-Mo1 2.205(5), B4-Mo2 2.277(6), B4-Mo1 2.342(5), Mo1-Mo2-Mo3 61.479(13), Mo2-Mo1-Mo3 61.752(13), Mo1-Mo3-Mo2 56.769(12).

The molecular structure of **4**, shown in Figure 2, can be seen as $[(\text{Cp}^*\text{Mo})_3(\mu\text{-H})_2(\mu_3\text{-H})(\mu\text{-CO})_2\text{B}_4\text{H}_4]$ which is fully consistent with the solution spectroscopic data. The polyhedral skeletal electron pair theory (PSEPT)^{23,33} showed that compound **4** can be viewed as 6 sep (skeletal electron pair) *oblato-nido* hexagonal bipyramidal cluster. As a result, the core geometry appears to be similar to $[(\text{Cp}^*\text{Mo})_2\text{B}_5\text{H}_9]$ (**I**)³⁴ where one of the $\{\text{BH}_2\}$ vertices in the open face has been replaced by isoelectronic fragment $\{\text{Cp}^*\text{Mo}(\text{CO})_2\}$. This resulted in a small stabilization of the LUMO but destabilization of the HOMO as compared to **I** (Table 1). Note that all the three Mo-Mo bond distances are dissimilar in **4**. Although, the axial Mo1-Mo2 distance is similar to that of **I** (2.833 vs 2.81 Å), the peripheral Mo-Mo distances are significantly

longer (3.004 and 2.946 Å). This has also been reflected in the WBI (Wiberg bond index) values; for example, WBI of Mo1-Mo2 (0.73) is ca. 1.5 times greater than the other Mo-Mo bonds (Mo2-Mo3: 0.39 and Mo1-Mo3: 0.51). The MO analyses of **4'** (a Cp analogue of **4**) show that both the HOMO and HOMO-1 (Figures 3b-c and S21) mostly involves Mo-Mo bonding. Further, to gain some insights into the Mo-Mo interactions in **4'** we have carried out the NBO analysis. The NLMOs clearly demonstrate the Mo-Mo interactions (Figures 3a and S22). The molecular graph, Laplacian plot of electron density and WBI values indicate that the CO ligands are closer to Mo3 that can also be seen from the X-ray structure analyses.

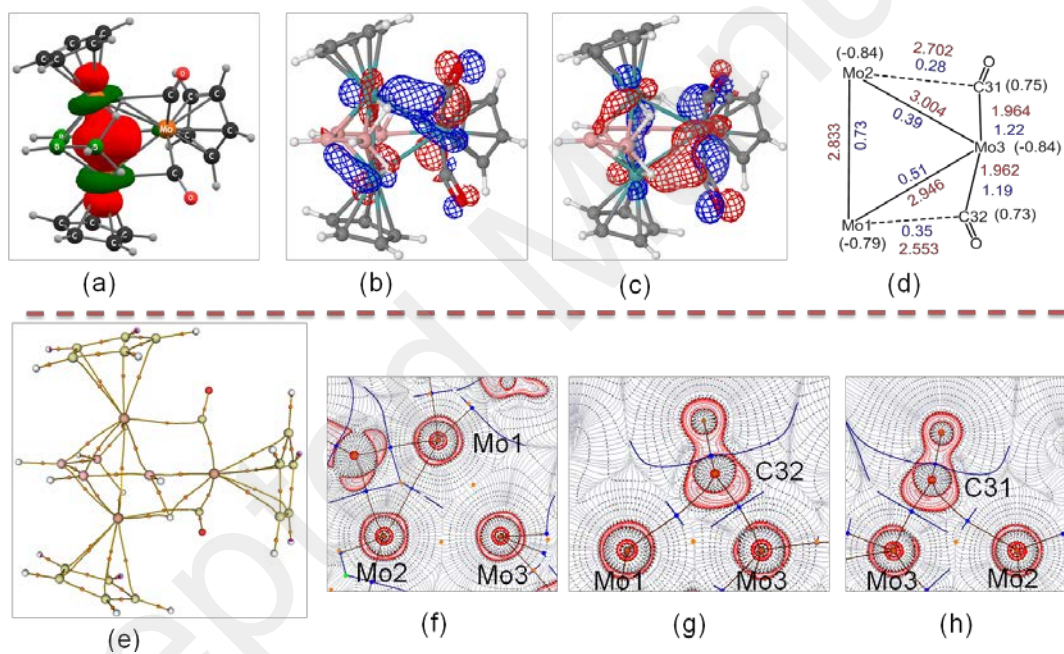
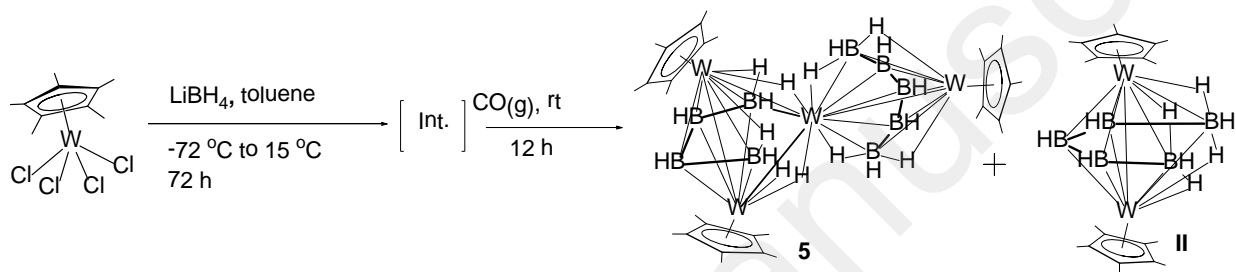


Figure 3. Investigating the Mo-Mo bonding in **4'**. (a) natural localized molecular orbital (NLMO) obtained from NBO analysis, (b) HOMO, (c) HOMO-1, (d) The Mo₃-core (WBIs are shown in blue, bond distances in red and natural charges in parenthesis), (e) molecular graphs for the model **1'**, contour line diagrams of the Laplacian of electron density in Mo₃ plane (f) and Mo-C-Mo planes (g-h) [Solid red lines indicate areas of charge concentration ($\nabla^2\rho(r) < 0$), while dashed black lines show areas of charge depletion ($\nabla^2\rho(r) > 0$)].

Table 1. DFT calculated energies of the HOMO and LUMO (eV), HOMO-LUMO gaps ($\Delta E = E_{\text{LUMO}} - E_{\text{HOMO}}$, eV) of $[(\text{CpM})_2\text{B}_5\text{H}_9]$ ($\text{M} = \text{Mo}(\text{I}')$ and $\text{W}(\text{II}')$), **3'**-**5'**, **7'** and **8'**.

	I'	II'	3'	4'	5'	7'	8'
HOMO	-4.40	-4.84	-4.99	-4.60	-4.84	-5.07	-3.52
LUMO	-1.32	-1.44	-3.25	-3.19	-2.99	-3.63	-1.10
ΔE	3.08	3.40	1.74	1.41	1.85	1.44	2.42



Scheme 2. Synthesis of tungstaborane cluster, **5**.

$[(\text{Cp}^*\text{M})_3\text{MB}_9\text{H}_{18}]$ [$\text{M} = \text{Mo}$ (**3**), W (**5**)]: Isolation and structural characterization of diborane(4) molybdenum complex **2** led us to explore the chemistry of tungsten system mainly with an objective to isolate the analogue of **2**, $\{\text{Cp}^*\text{W}(\text{CO})_2\}_2\text{B}_2\text{H}_4$. Although the objective of isolating analogous **2** was not achieved, we have isolated a vertex-fused tungsten cluster $[(\text{Cp}^*\text{W})_3\text{WB}_9\text{H}_{18}]$ (**5**). Compound **5** was isolated as a byproduct in parallel to the formation of $[(\text{Cp}^*\text{W})_2\text{B}_5\text{H}_9]$ (**II**).³⁵ These compounds can be separated by preparative thin-layer chromatography (TLC), allowing the characterization of pure **5**. The mass spectrum of **5** showed a molecular ion peak $[m/z]$ corresponding to $\text{C}_{30}\text{H}_{63}\text{W}_4\text{B}_9$, while the IR spectrum confirms the absence of CO ligands. The $^{11}\text{B}\{^1\text{H}\}$ NMR spectrum displayed a set of nine resonances between $\delta = 55.3$ and 21.9 ppm (from high frequency to low frequency), distributed over a chemical shift range of *ca.* 30 ppm.³⁶ Besides the BH terminal protons, the ^1H NMR showed highly shielded upfield resonances which may be due to the presence of bridging W-H-B protons. In addition,

the ^1H and ^{13}C NMR spectra of **5** are in consistent with the existence of two chemically different Cp* ligands.

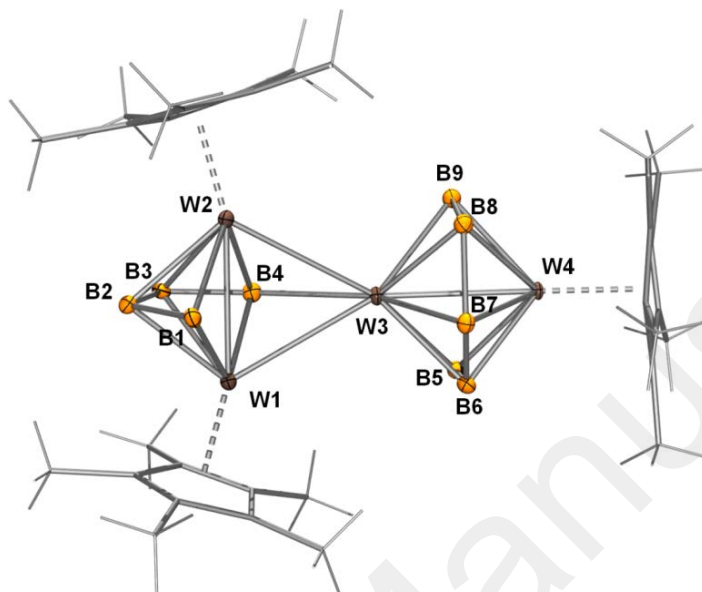


Figure 4. Molecular structure of **5**. Ellipsoids are set at 30% probability (hydrogen atoms on the Cp* ligands are omitted for clarity) Selected bond lengths (Å) and bond angles (degree): W1-W2 2.839(2), W1-W3 3.013(2), W3-W4 2.856(2), W2-W3 3.046(2), W1-B1 2.258(4), W1-B4 2.6181(5), B1-B2 1.699(6), B2-B3 1.760(6), B8-B9 1.838(8), B7-B8 1.770(8), W1-W3-W2 55.8(5), W1-W2-W3 61.4(5), W2-W1-W3 62.6(5), W1-B1-W2 77.1(13), B1-B2-B3 120.0(3).

The single crystal X-ray structure analysis was performed on a brown crystal of **5** that was obtained from the concentrated hexane solution at $-4\text{ }^{\circ}\text{C}$. As shown in Figure 4, the molecular structure of **5** can be viewed as a fusion of two clusters through a common single atom vertex. The X-ray structure and the solution state spectroscopic data are consistent with the molybdenum analogue, $[(\text{Cp}^*\text{Mo})_3\text{MoB}_9\text{H}_{18}]$ (**3**).²⁸ Although, all the hydrogen atoms were not located in the X-ray diffraction study, evidence for their presence has been unequivocally supported by ^1H NMR spectroscopy. Core structure of **5** is composed of two independent

clusters, *oblato-nido* $\{W_2B_5\}$ and *oblato-arachno* $\{W_2B_4\}$ hexagonal bipyramid clusters fused in perpendicular fashion through a naked tungsten atom (W3). The dihedral angle between the basal planes of the corresponding B_5 - and B_4 - belts is 85.53° . This brings six B atoms and four hydride ligands in the coordination sphere of W3 in expense of a Cp^* ligand of compound **II**. Both the cluster fragments and their structural parameters resemble with those of **II**. However, the solid state X-ray structure reveals two different sets of W-W bond lengths [W1-W2: 2.839(2), W3-W4 (2.856(2) Å and W1-W3: 3.013(2), W2-W3: 3.046(2) Å] with the average W-B and B-B bond distances comparable with the reported tungstaborane compounds (Table 2). Longer W-W bond lengths may be attributed to the unique chemical environment of the naked W3. This observation is in line with the Laplacian plot (Figure 5b) as well as ELF plot (Figure 5c), as both the diagrams reveal high electron density concentration along W1-W2 bond than W1-W3 and W2-W3. Similar bonding situation has been observed in $[1-(Cp^*Ru)(\mu-H)B_4H_9]_2Ru$ that showed shorter metal-metal bond distance compared to $[1,2-(Cp^*Ru)_2(\mu-H)B_4H_9]$.³⁷ The only difference between **3** and **5** is their ^{11}B NMR chemical shifts. The ^{11}B resonances of **5** appeared at upfield region as compared to **3**. This can well be understood from the fact that more charge accumulation occurred over B centers in **5** compare to **3** (Figure 5e).

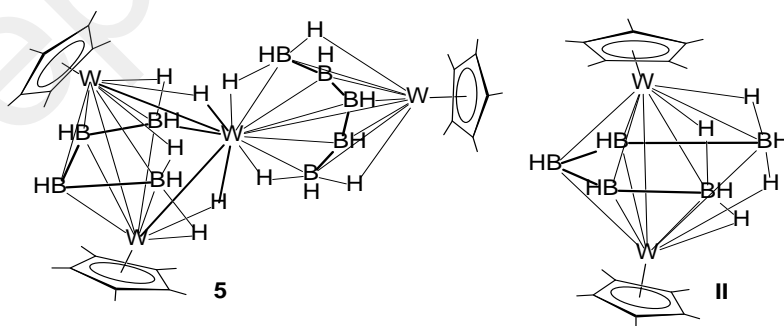
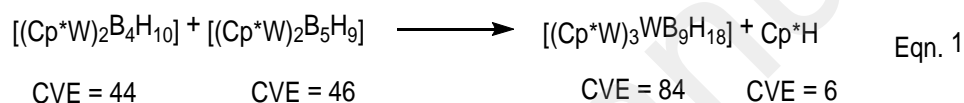


Chart 2. Structural equivalence of **5** with **(II)**.

The 18-electron count rule for **5** becomes more apparent when one considers that the W atom in $[(\text{Cp}^*\text{W})_2\text{B}_5\text{H}_9]$ (**II**, Chart 2) receives five electrons from the Cp^* ligand. This is comparable to a case in which $\{(\text{Cp}^*\text{W})_2\text{B}_4\text{H}_9\}$ fragment in **5** contributes five electron to the bare tungsten atom (W3, Figure 4). Thus, the replacement of one of the Cp^* ligands from **II** with a five electron donor fragment $\{(\text{Cp}^*\text{W})_2\text{B}_4\text{H}_9\}$, the 18-electron count for the bare W atom satisfied and hence this may be considered as an analogue to **II**. Both the NBO and MO analysis of **5** and **II** support these arguments (Figures 5a,d and S23-S24). Further, the HOMO shows large localization of electron density on the metal centers (Figure 5a and S23).



Cluster condensation or fusion by vertex, edge, or face sharing is quite familiar in polyhedral borane, metallaborane and carborane chemistry.³⁸ Electron counting of these types of clusters can well be understood following Mingos's fusion formalism^{38f} and Jemmis's mno rule.²⁴ Existence of cluster **II** led us to propose a plausible pathway for the formation of compound **5**. From Eqn 1, it is reasonable to assume that, during the progress of the reaction, $[(\text{Cp}^*\text{W})_2\text{B}_4\text{H}_{10}]$ and **II** underwent a cluster condensation reaction to produce **5** with the elimination of a Cp^* . As a result $\{(\text{Cp}^*\text{W})_2\text{B}_4\text{H}_9\}$ acts as a ligand for the formation of $\{(\text{Cp}^*\text{W})\text{WB}_5\text{H}_9\}$ (Chart 1).³⁹

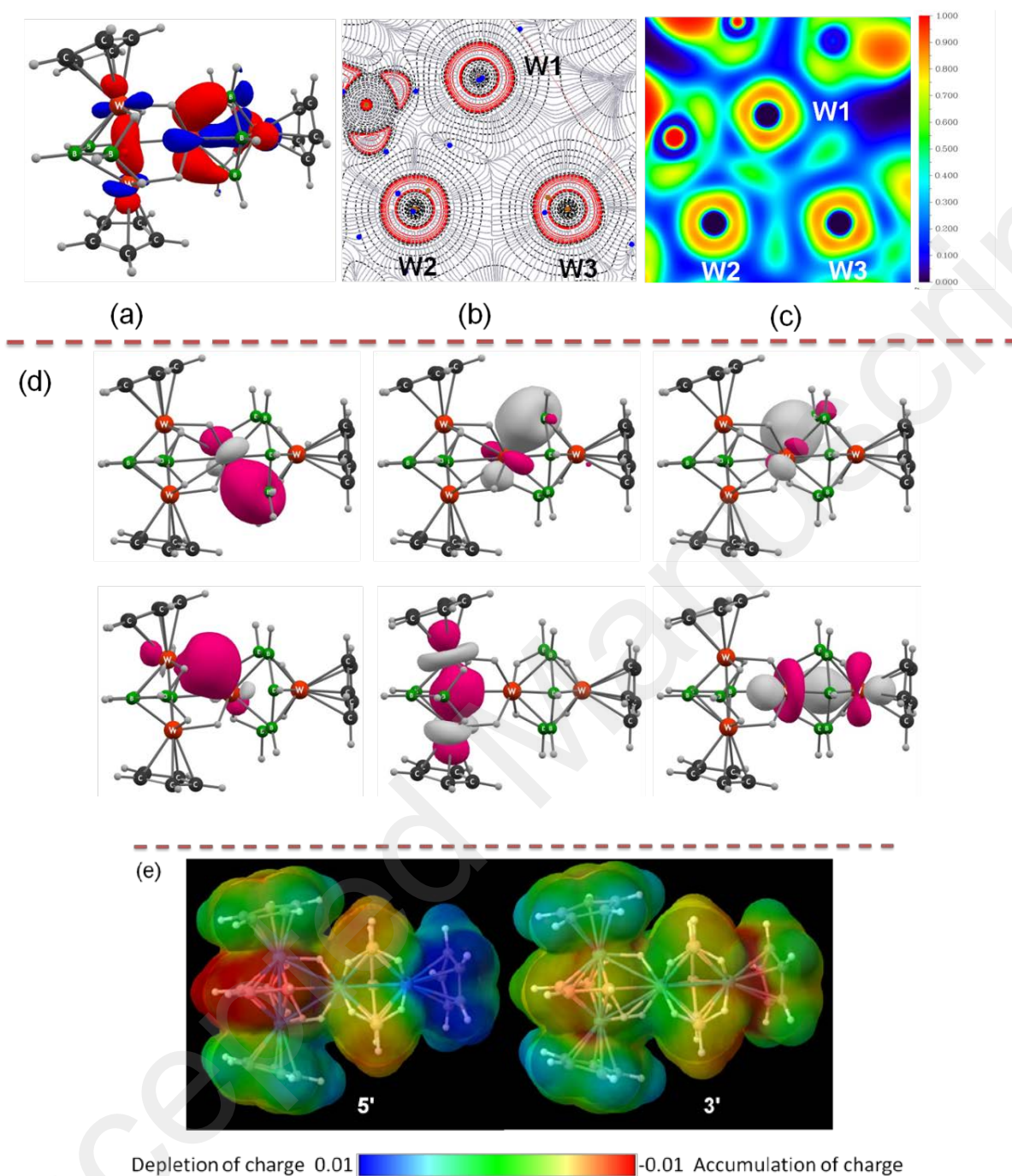
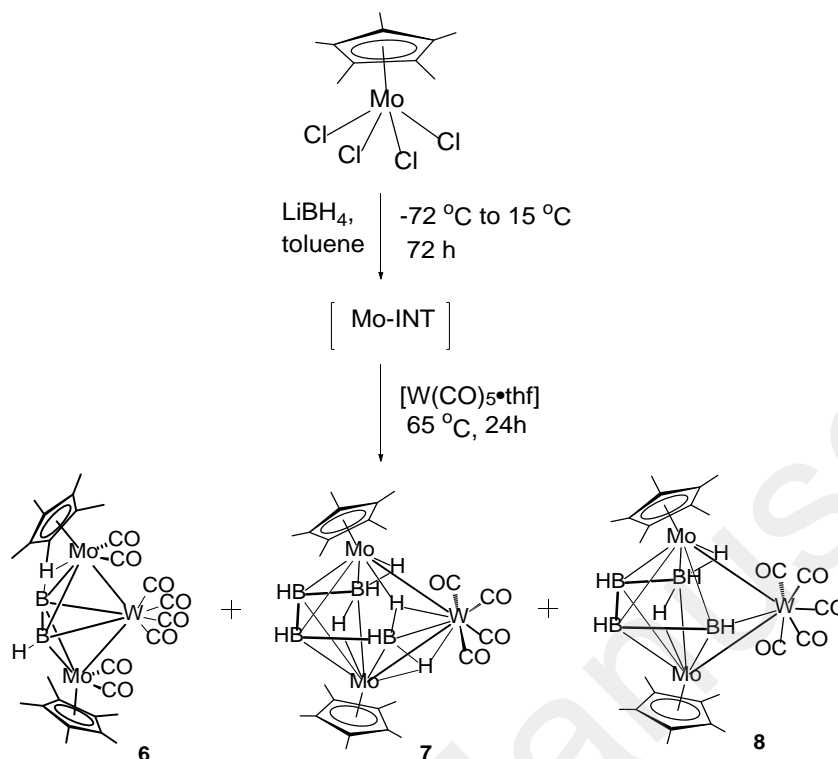


Figure 5. Bonding analyses of **5'** [(a) shows the HOMO, (b) contour line diagram of the Laplacian of electron density in the plane of W1-W2-W3, (c) showing ELF plot in the plane of W1-W2-W3, (d) selected natural localized molecular orbital (NLMO) obtained from NBO analysis, (e) Electrostatic potential analysis].



Scheme 3. Synthesis of diborene(2), (**6**) and heterometallaboranes (**7** and **8**). $[\text{Mo-INT}]$ is an *insitu* generated intermediate, obtained from the reaction of $[\text{Cp}^*\text{MoCl}_4]$ and $[\text{LiBH}_4]$ at -72°C .

$[(\text{Cp}^*\text{Mo})_2\text{B}_4\text{H}_8\text{W(CO)}_4]$, **7 and $[(\text{Cp}^*\text{Mo})_2\text{B}_4\text{H}_6\text{W(CO)}_5]$, **8**:** In order to replace $\{\text{Cp}^*\text{Mo(CO)}_2\text{H}\}$ unit in **4** with $\{\text{W(CO)}_5\}$, we treated the intermediate, obtained from the reaction of $[\text{Cp}^*\text{MoCl}_4]$ and $[\text{LiBH}_4]$, with $\{\text{W(CO)}_5\cdot\text{thf}\}$. The reaction yielded two trimetallic clusters $[(\text{Cp}^*\text{Mo})_2\text{B}_4\text{H}_8\cdot\text{W(CO)}_4]$, **7** and $[(\text{Cp}^*\text{Mo})_2\text{B}_4\text{H}_6\text{W(CO)}_5]$, **8** along with the formation of diborene(2) complex, $[\{\text{Cp}^*\text{Mo(CO)}_2\}_2\text{B}_2\text{H}_2\text{W(CO)}_4]$ (**6**), reported recently in a communication.¹⁸ Since the landmark report of N-heterocyclic carbene (NHCs) stabilized diborene compounds by Robinson, the chemistry of unsaturated boron-boron species has extended significantly and in this respect, **6** is an exceptional entry to this diborene(2) species.^{40,41} Compounds **7** and **8** were isolated as brown and green solids in moderate yields.

Room temperature $^{11}\text{B}\{^1\text{H}\}$ NMR of compounds **7** and **8** appeared between $\delta = 27$ and 103 ppm (from high frequency to low frequency), with signals of **8** being relatively downfield shifted. The IR spectra of both **7** and **8** showed the stretching frequencies corresponding to the CO ligands and BH_t . The ^1H NMR spectra of **7** and **8** reveal the presence of one equivalent of Cp^* proton. Further, the mass spectrometric data suggest a close association between compounds **7** and **8**.

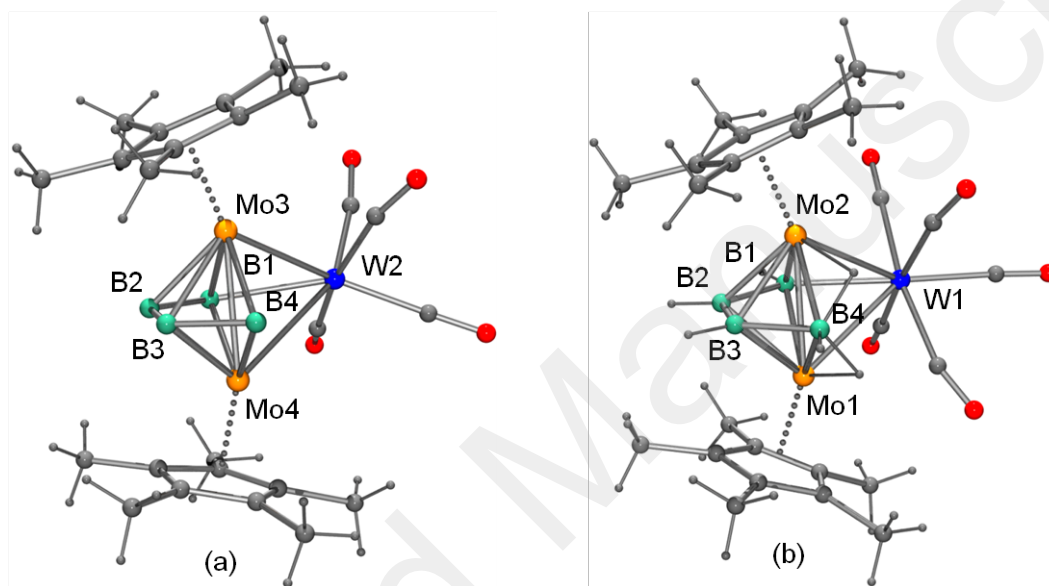


Figure 6. Molecular structure of (a) **7** and (b) **8**. Bridging hydride ligands and the hydrogen atoms attached to the boron atoms of **7** could not be located. Selected bond lengths (\AA) and bond angles ($^\circ$). **7**: Mo3-B2 2.1821(15), Mo3-B3 2.2380(16), Mo3-B4 2.2671(16), Mo3-B1 2.2841(16), Mo3-Mo4 2.8275(18), Mo3-W2 2.9908(15), W2-B4 2.3955(7), B1-B2 1.7399(3), B2-B3 1.7185(6), B3-B4 1.7003(7). Mo4-W2-Mo3 55.95(4), Mo3-B1-Mo4 75.87(5), Mo3-B4-Mo4 75.73(5), **8**: B1-B2 1.706(5), B1-Mo1 2.283(3), B1-W1 2.315(3), B2-B3 1.739(5), B2-Mo1 2.175(3), B3-B4 1.744(5), B3-Mo2 2.180(4), B4-Mo2 2.309(3), Mo1-W1 2.9801(3), Mo1-Mo2 2.8308(3), Mo2-B1-Mo1 77.17(10), B1-W1-Mo1 49.13(8), Mo1-W1-Mo2 56.588(7).

Single crystals of **7** and **8** suitable for X-ray diffraction were grown from hexane at -10 °C. The solid-state X-ray structures of **7** and **8**, shown in Figures 6 (a) and 7(b) respectively, are consistent with the spectroscopic data. The core geometries are analogous to $[(Cp^*Cr)_2B_4H_8Fe(CO)_3]$ and $[(Cp^*Cr)_2Co-(CO)_3B_4H_7]$.⁴² Note that, the hydrogen atoms attached to boron could not be located by solid state X-ray diffraction study of **7**⁴³, however their positions were fixed based on ¹H NMR as shown in Scheme 3. As $\{W(CO)_4\}$ and $\{W(CO)_5\}$ are isolobal to (BH_3) and (BH) , compounds **7** and **8** are formally related to 46 cve (cluster valance electron) cluster **I**. Thus, the core geometries of **7** and **8** can be viewed as a 6 *sep* oblatonido hexagonal bipyramid or $\{Mo_2B_3H_3\}$ trigonal-bipyramidal core face capped by (BH_3) and $\{W(CO)_4\}$ or $\{W(CO)_5\}$ fragments. The Mo-Mo bond distances in **7**, **8** and **I** are comparable (**7**: 2.8275(18), **8**: 2.8308(3), $[(Cp^*Mo)_2B_5H_5(\mu-H)_4]$: 2.80 Å; Table 2), however they are shorter than those observed in $[CpMo(CO)_3]_2$ (3.22 Å) and $[Mo_2(CO)_{10}]^{2-}$ (3.123 Å).⁴⁴

The HOMO and HOMO-1 of **8'** (Figures 7b and c) shows electron localization over the metal centres. The HOMO, in particular, shows that the $\{W(CO)_5\}$ fragment interacts through its half occupied π -symmetry orbital. The empty σ orbital of the $\{W(CO)_5\}$ fragment interacts with a low lying filled Cp^*Mo orbital leading to donor-acceptor interactions (Figures S26-S27). This was further supported by the electron density distribution analysis where the Laplacian plot showed more electron density along the Mo1-Mo2 than W1-Mo1/Mo2 (Figure 7f). As a result, the W centre attains the 18-electron rule. In addition, the MO analyses (HOMO and HOMO-1, Figures 7b and c, respectively) demonstrate weak interactions between the Mo based d orbitals and π^* of the CO ligands that established the weak nature of Mo-CO interactions and more like terminal to W1 centre. This observation was also supported by the WBI values and the molecular graphs (Figures 7d-e). On the other hand, the $[W(CO)_4]$ moiety in **7** attached to $[(Cp^*Mo)_2B_4H_8]$

through two face-bridging hydrogen and a pair of Mo-W interactions (Figure S25). An interesting statement that can be concluded from the NBO charge analysis of **8'** is the diverse oxidation states of the metal centres. The comparatively reduced oxidation state of W1 (natural charge -1.57, whereas that of Mo centres are -0.87 and -0.84) indicates the flow of electron density predominantly towards W1 centre. This further supports the acceptor behaviour of $[\text{W}(\text{CO})_5]$ moiety.

Table 2. Selected structural parameters of **7** and **8** and other related compounds.

Compounds	sep	$d(\text{M-M})$ (Å)	$d(\text{M-B})$ (Å) ^a	$d(\text{B-B})$ (Å) ^a
$[(\text{Cp}^*\text{Cr})_2\text{B}_4\text{H}_8\text{Fe}(\text{CO})_3]$	6	2.71 ^a	2.15	1.72
$[(\text{Cp}^*\text{Cr})_2\text{Co}(\text{CO})_3\text{B}_4\text{H}_7]$	6	2.69 ^b	2.13	1.69
$[(\text{Cp}'\text{Mo})_2\text{B}_5\text{H}_5(\mu\text{-H})_4]$	6	2.81	2.26	1.73
$[(\text{Cp}'\text{W})_2\text{B}_5\text{H}_5(\mu\text{-H})_4]$	6	2.82	2.26	1.71
$[(\text{Cp}^*\text{Mo})_2\text{B}_5\text{H}_9\text{Fe}(\text{CO})_3]$	7	2.94 ^c	1.75	1.76
$[(\text{Cp}'\text{W})_2\text{B}_5\text{H}_9\text{Fe}(\text{CO})_3]$	7	2.93 ^d	1.79	1.77
7	6	2.83	2.24	1.72
8	6	2.83	2.24	1.73

^a average distance, $\text{Cp}' = (\eta^5\text{-MeC}_5\text{H}_4)$

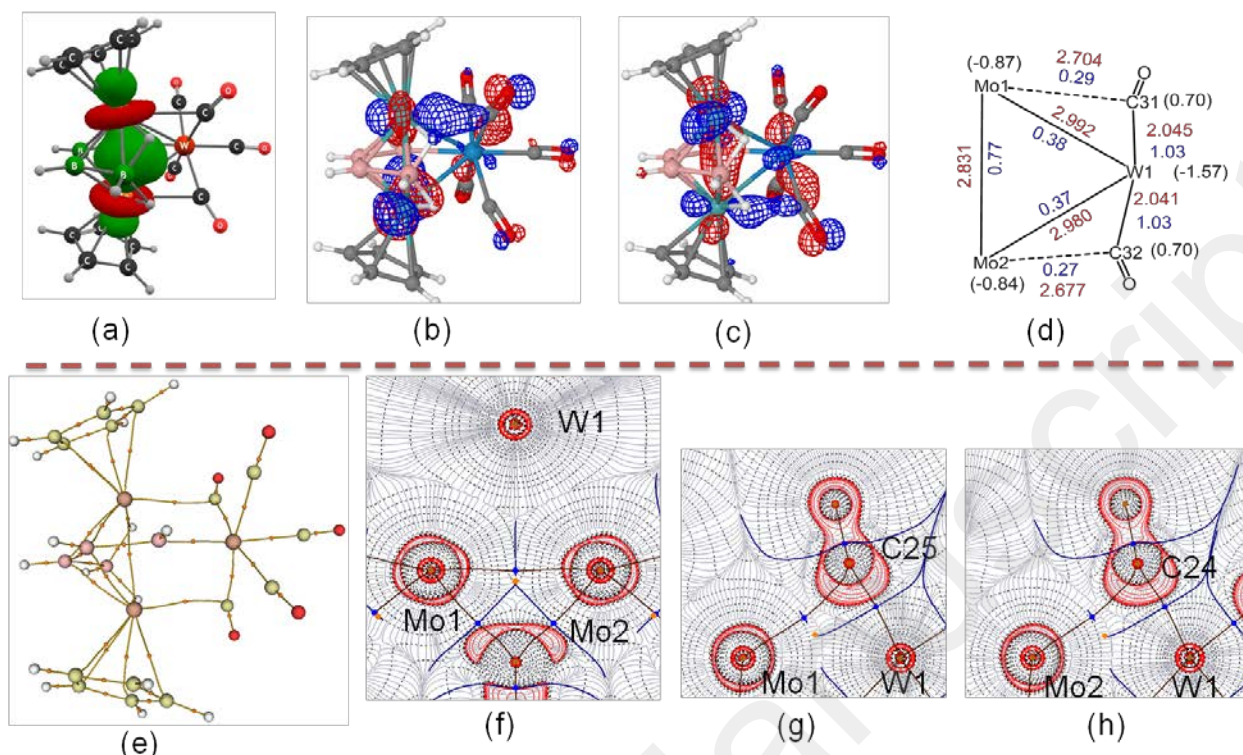


Figure 7. Mo-Mo bonding in **8'** (Cp analogue of **8**). (a) natural localized molecular orbital (NLMO) obtained from NBO analysis, (b) HOMO, (c) HOMO-1, (d) The Mo₃-core (WBIs are shown in blue, bond distances in red and natural charges in parenthesis), (e) molecular graphs for the model **8'**, contour line diagrams of the Laplacian of electron density in Mo₃ plane and (f) Mo-C-Mo planes (g-h) [solid red lines indicate areas of charge concentration ($\nabla^2\rho(r) < 0$), while dashed black lines show areas of charge depletion ($\nabla^2\rho(r) > 0$)].

CONCLUSION

In summary, we have described the synthesis of molybdenum diborane(4) complex, $[\{\text{Cp}^*\text{Mo}(\text{CO})_2\}_2\{\mu\text{-}\eta^2\text{:}\eta^2\text{-B}_2\text{H}_4\}]$ (**2**) that not only shows the presence of unique B₂H₄ of C_s type, it also mimics Cotton's dimolybdenum-acetylene complex, $[\{\text{CpMo}(\text{CO})_2\}_2\text{C}_2\text{H}_2]$. Our pursuit of growing the library of this type of complexes led us to isolate homoleptic molybdaboranes, $[(\text{Cp}^*\text{Mo})_3(\mu\text{-H})_2(\mu_3\text{-H})(\mu\text{-CO})_2\text{B}_4\text{H}_4]$ (**4**) and a vertex-fused cluster,

$[(\text{Cp}^*\text{W})_3\text{WB}_9\text{H}_{18}]$ (**5**). Further, we have described the synthesis of two mixed metallaboranes, $[(\text{Cp}^*\text{Mo})_2\text{B}_4\text{H}_8\text{W}(\text{CO})_4]$ (**7**) and $[(\text{Cp}^*\text{Mo})_2\text{B}_4\text{H}_6\text{W}(\text{CO})_5]$ (**8**) along with diborene(2) complex, $[(\text{Cp}^*\text{Mo}(\text{CO})_2)_2\text{B}_2\text{H}_2\text{W}(\text{CO})_4]$ (**6**). Electron counting as well as molecular orbital analyses suggest that metallaboranes **7** and **8** are the analogues of parent $[(\text{Cp}^*\text{Mo})_2\text{B}_5\text{H}_9]$ cluster. These results exemplify the presence of multimetallic molecular clusters with exciting geometry and bonding.

EXPERIMENTAL SECTION

General Procedures and Instrumentation. All the manipulations were conducted under an atmosphere of dry argon or in vacuo using standard Schlenk line or glove box techniques. Solvents (hexane, toluene, thf) were purified by distillation from appropriate drying agents- (sodium/benzophenone) under dry argon prior to use. CDCl_3 and C_6D_6 were degassed by three freeze-pump-thaw cycles and stored over molecular sieves. Compounds $[\text{Cp}^*\text{MCl}_4]$ ($\text{M} = \text{Mo}$ and W), $[\text{M}'(\text{CO})_5.\text{thf}]$, ($\text{M}' = \text{Cr}, \text{Mo}$ and W) were prepared according to literature method,⁴⁵ while other chemicals such as, $[\text{LiBH}_4.\text{thf}]$ 2.0 M in THF, Cp^*H , $n\text{-BuLi}$, $[\text{Cr}(\text{CO})_6]$, $[\text{Mo}(\text{CO})_6]$ and $[\text{W}(\text{CO})_6]$ were obtained commercially (Aldrich) and used as received. MeI was purchased from Aldrich and freshly distilled prior to use. The external reference for the ^{11}B NMR, $[\text{Bu}_4\text{N}(\text{B}_3\text{H}_8)]$ was synthesized with the literature method.⁴⁶ Preparative thin layer chromatography was performed with Merck 105554 TLC silica gel 60 F₂₅₄, layer thickness 250 μm on aluminium sheets (20x20 cm). NMR spectra were recorded on 400 and 500 MHz Bruker FT-NMR spectrometers. The residual solvent protons were used as reference (δ , ppm, d_6 -benzene, 7.16, CDCl_3 , 7.26), while a sealed tube containing $[\text{Bu}_4\text{N}(\text{B}_3\text{H}_8)]$ in d_6 -benzene (δ_{B} , ppm, -30.07) was used as an external reference for the ^{11}B NMR. The infrared spectra were recorded on a Nicolet iS10 spectrometer. Electrospray mass (ESI-MS) spectra were recorded on

a Qtof Micro YA263. The photo-reactions described in this report were conducted in a Luzchem LZC-4 V photo reactor, with irradiation at 254–350 nm. MALDI-TOF mass spectra were recorded on a Bruker Ultraflextreme by using 2,5-dihydroxybenzoic acid as a matrix and a ground steel target plate and CH analyses were obtained on Perkin Elmer Instruments series II model 2400.

Synthesis of 4: A solution of **1** (0.140 g, 0.25 mmol) in toluene was treated with carbon monoxide over a period of 15 mins and the reaction mixture was stirred for 12 h at ambient temperature. The solvent was evaporated in vacuo and the crude was extracted with hexane:CH₂Cl₂ (80:20) solvent mixture and filtered through a frit using celite. After removal of solvent from the filtrate, the residue was subjected to chromatographic work-up using silica gel TLC plates. Elution with hexane:CH₂Cl₂ (75:25) solvent mixture afforded yellow **2** (0.052 g, 32 %),¹⁸ brown **3** (0.035 g, 15.4 %) and brown **4** (0.020 g, 10%).

4: HRMS (ESI⁺): *m/z* calculated for [C₃₂H₅₂B₄Mo₃O₂+H]⁺: 807.1579; found 807.1588; ¹¹B{¹H} NMR (22 °C, 128 MHz, CDCl₃): δ = 23.5 (br, 1B), 46.3 (br, 1B), 83.2 (br, 1B), 88.8 (br, 1B), ¹H NMR (22 °C, 500 MHz, CDCl₃): δ = 4.82 (br, 4H, BH), 1.95 (s, 15H, 1Cp*), 1.91 (s, 30H, 2Cp*), -8.85, -9.35, -13.17 (br, 3H, Mo–H–B); ¹³C{¹H} NMR (22 °C, 125 MHz, CDCl₃): δ = 187.2, 183.9 (CO), 102.4, 100.2 (C₅Me₅), 13.0, 10.8 (C₅Me₅); IR (hexane) ν/cm⁻¹: 2420(BH), 1787(CO), 1729 (CO).

Synthesis of 5: In a flame-dried Schlenk tube [Cp*WCl₄] (0.1 g, 0.22 mmol) in 15 mL of toluene was treated with 5-fold excess of [LiBH₄.THF] (0.55 mL, 1.1 mmol) at -40°C and allowed to stir at allowed to stir at 10 °C for 48 hour. In the reaction mixture CO(g) passed for 12 hour at room temperature. After removal of toluene, the residue was extracted into hexane and

filtered through a frit using Celite. After removal of solvent from the filtrate, the residue was subjected to chromatographic workup using silica gel TLC plates. Elution with a hexane/CH₂Cl₂ (75:15 v/v) mixture yielded brown **5** (0.030 g, 10.9%) along with known [(Cp*W)₂B₅H₉] (0.048 g, 31%).

5: HRMS (ESI⁺): *m/z* calculated for [C₃₀H₆₃B₉W₄+H]⁺: 1259.3883; found 1259.3915; . ¹¹B{¹H} NMR (22 °C, 128 MHz, CDCl₃): δ = 55.3 (br, 1B), 51.0 (br, 1B), 47.8 (br, 1B), 45.8 (br, 1B), 44.6 (br, 1B), 40.7 (br, 1B), 27.6 (br, 1B), 24.5 (br, 1B), 21.9 (br, 1B). ¹H NMR (22 °C, 500 MHz, CDCl₃): δ = 6.19 (br, BH_i), 2.22 (s, 15H, 1Cp*), 2.20 (s, 15H, 1Cp*) 2.19 (s, 15H, 1Cp*), -1.79 (br, 1H, B–H–B), -3.61 (br, 1H, B–H–B), -7.58 (br, 1H, W–H–B), -8.56 (br, 2H, W–H–B), -9.58 (br, 1H, W–H–B), -10.64 (br, 1H, W–H–B), -13.08 (br, 1H, W–H–B). ¹³C{¹H} NMR (22 °C, 100 MHz, CDCl₃): δ = 108.8 (C₅Me₅), 107.2 (C₅Me₅), 12.6 (C₅Me₅), 11.6 (C₅Me₅). IR (hexane) ν/cm⁻¹: 2473(BH_i).

Synthesis of 7 and 8: In a flame-dried Schlenk tube [Cp*MoCl₄], (0.1 g, 0.27 mmol) in 10 mL of toluene was treated with 5-fold excess of [LiBH₄.THF] (0.7 mL, 1.4 mmol) at -40°C and allowed to stir at room temperature for one hour. After removal of toluene, the residue was extracted into hexane and filtered through a frit using Celite. The brownish-green hexane extract was dried in vacuo, and taken in 10 mL of THF and heated at 65°C with [W(CO)₅.THF] for 24 hours. The solvent was evaporated in vacuo and residue was extracted into hexane and passed through celite. After removal of solvent from the filtrate, the residue was subjected to chromatographic workup using silica gel TLC plates. Elution with a hexane/CH₂Cl₂ (80:10 v/v) mixture yielded dark brown **7** (0.025 g, 11.4%) and green **8** (0.025 g, 11%).

7: HRMS (ESI⁺): m/z calculated for [C₂₄H₃₈B₄O₄Mo₂W₁+Na]⁺: 837.0657; found 837.0647; ¹¹B{¹H} NMR (22 °C, 128 MHz, CDCl₃): δ = 27.9 (br, 1B), 41.9 (br, 1B), 81.2 (br, 2B); ¹H NMR (22 °C, 400 MHz, CDCl₃): δ = 4.46, (br, BH_l), 2.03 (s, 30H, 2Cp*), -6.90 (br, 2H, Mo–H–B), -10.17 (br, 1H, W–H–B), -13.32 (br, 1H, Mo–H–W); ¹³C{¹H} NMR (22 °C, 100 MHz, CDCl₃): δ =195.4, 189.4, 181.7 (CO), 98.9 (C₅Me₅), 10.9 (C₅Me₅); IR (hexane) ν /cm⁻¹: 2474 (BH_l), 2008(CO), 1937(CO), 1878 (CO)

8: HRMS (ESI⁺): m/z calculated for [C₂₅H₃₆B₄O₅Mo₂W₁+H]⁺: 841.0630; found 841.0623; ¹¹B{¹H} NMR (22 °C, 128 MHz, CDCl₃): δ = 103.0(br, 2B), 77.9 (br, 1B), 77.0 (br, 1B); ¹H NMR (22 °C, 400 MHz, CDCl₃): δ = 5.87, (br, BH_l), 1.93 (s, 30H, 2Cp*), -6.55 (br, 1H, Mo–H–B), -7.35 (br, 1H, Mo–H–B); ¹³C{¹H} NMR (22 °C, 100 MHz, [D₆]-benzene): δ =198.6, 192.9 (CO), 108.5 (C₅Me₅), 12.9 (C₅Me₅); IR (hexane) ν /cm⁻¹: 2498 (BH_l), 2043 (CO), 2008(CO), 1969 (CO), 1890(CO).

Computational details. Geometry optimizations and electronic structure calculations were carried out on Gaussian09 (rev. C.01)⁴⁷ program package using BP86 functional⁴⁸ and def2-TZV⁴⁹ basis set from EMSL Basis Set Exchange Library. The 28 core electrons of molybdenum and tungsten were replaced by the quasi-relativistic effective core potential def2-ECP.⁵⁰ Vibrational analyses were carried out for all structures, and the absence of any imaginary frequency confirmed that all structures represent minima on the potential energy hypersurface. The NMR chemical shifts were calculated on the BP86/def2-TZVP optimized geometries using the hybrid Becke–Lee–Yang–Parr (B3LYP) functional and aforementioned basis set.⁵¹ The NMR calculation utilized gauge-including atomic orbitals (GIAOs) method.⁵² The ¹¹B NMR chemical shifts were calculated relative to B₂H₆ (B3LYP B shielding constant 84.23 ppm) and converted to the usual [BF₃.OEt₂] scale using the experimental $\delta(^{11}\text{B})$ value of B₂H₆, 16.6 ppm.

Natural bonding analyses were performed with the natural bond orbital (NBO) partitioning scheme as implemented in the Gaussian 09 suite of programs.⁵³ Wiberg bond indexes (WBI) were obtained on natural bond orbital analysis.⁵⁴ In order to understand the nature of bonding of the synthesized molecules in greater detail, the topological properties of the resultant electron density, ρ , obtained from the wave functions of all the optimized structures were analyzed with the quantum theory of atoms in molecules (QTAIM).⁵⁵ The QTAIM analysis were carried out utilizing Multiwfn V.3.3.8 package⁵⁶ whereas the wave functions were generated with Gaussian09 at the same level of theory as was used for geometry.

X-ray Structure Determination. Crystal data for **4**, **5** and **8** were collected and integrated using Bruker Kappa apexII CCD single crystal diffractometer and for **7** with OXFORD Diffraction SUPER NOVA CCD Diffractometer, equipped with graphite monochromated Mo-K α (λ = 0.71073 Å) radiation. Data collection for **4** and **8** were carried out at 296 K and for **5** and **7** at 293 K, using ω - ϕ scan modes. Multi-scan absorption correction has been employed for the data using SADABS⁵⁷ program. The structures were solved by heavy atom methods using SHELXS-97 or SIR92⁵⁸ and refined using SHELXL-2014.⁵⁹ These data can be obtained free of charge from The Cambridge Crystallographic Data Centre via [www.ccdc.cam.ac.uk/ data_request/cif](http://www.ccdc.cam.ac.uk/data_request/cif)

ASSOCIATED CONTENT

Supporting Information. The Supporting Information is available free of charge on the ACS Publications website.

Spectroscopic data for **4-5** and **7-8**; optimized geometries and MO diagrams (PDF).


CCDC 1878369 (**4**), 1878370 (**5**) 1878367 (**7**) and 1878368 (**8**) contain the supplementary crystallographic data for this paper. These data can be obtained free of charge via

www.ccdc.cam.ac.uk/data_request/cif, or by emailing data_request@ccdc.cam.ac.uk, or by contacting The Cambridge Crystallographic Data Centre, 12 Union Road, Cambridge CB2 1EZ, UK; fax: +44 1223 336033

AUTHOR INFORMATION

Corresponding Author

*E-mail: sghosh@iitm.ac.in. Tel: +91-44-22574230. Fax: +91 44-22574202

ORCID  0000-0001-6089-8244

Notes

The authors declare no competing financial interest.

ACKNOWLEDGMENT

The authors acknowledge the Council of Scientific & Industrial Research (CSIR) (Project No. 01(2939)/18/emr-ii), New Delhi, India for financial support. R.B thanks IIT Madras for research fellowship.

REFERENCES

- (1) (a) Stock, A. Hydrides of Boron and Silicon. Cornell University Press, Ithaca, New York, **1933**. (b) Greenwood, N. N.; Earnshaw, A. Chemistry of the Elements (2nd ed.). Butterworth-Heinemann, Ed. **1997**.
- (2) (a) Handbook of Boron Science: With Application in Organometallics, Catalysis, Materials and Medicines, Hosmane, N.S.; Eagling, R. Eds. *World Scientific*, **2018**. (b) Boron and

Gadolinium Neutron Capture Therapy for Cancer Treatment, Hosmane, N. S.; Maguire, J. A.; Zhu, Y.; Takagaki, M. *World Scientific*, **2012**.

(3) Reed, C. A. Carborane acids. New “strong yet gentle” acids for organic and inorganic chemistry. *Chem. Commun.* **2005**, 1669–1677.

(4) (a) Plešek, J. Potential applications of the boron cluster compounds. *Chem. Rev.* **1992**, 92, 269-278. (b) Lu, X.; Shao, L.; Wang, X.; Chen, Q.; Liu, J.; Chu, W-K. Shallow Junction Formation By Small Cluster Implantation. *Proc. Electrochem. Soc.* **2001**, 2001-9, 337-344. (c) Baše, T.; Bastl, Z.; Šlouf, M.; Klementová, M.; Šubrt, J.; Vetushka, A.; Ledinský, M.; Fejfar, A.; Macháček, J.; Carr, M. J.; Londesborough, M. G. S. Gold Micrometer Crystals Modified with Carboranethiol Derivatives. *J. Phys. Chem. C* **2008**, 112, 14446-14455.

(5) (a) Barton, L.; Srivastava, S. K. in *Comprehensive Organometallic Chemistry II*, Vol. 1 Wilkinson, G.; Abel, E. W.; Stone, F. G. A. Eds. chap. 8. boranes and mimicking *Pergamon*, New York, **1995**. (b) Fehlner, T. P. Borane Mimics of C₁-M_m Organometallic Complexes. *Angew. Chem. Int. Ed.* **2005**, 44, 2056-2058. (c) Mondal, B.; Borthakur, R.; Ghosh, S. Organometallic Chemistry and Catalysis of Transition Metal–Borane Compounds, Vol. 2, Ch. 7 in *Handbook of Boron Science: With Application in Organometallics, Catalysis, Materials and Medicines*, Hosmane, N. S.; Eagling, R. Eds. *World Scientific*, **2018**.

(6) (a) Longuet-Higgins, H. C.; Bell, R. P. The structure of the boron hydrides. *J. Chem. Soc.* **1943**, 250-255. (b) Laszlo, P. A. Diborane Story. *Angew. Chem. Int. Ed.* **2000**, 39, 2071-2072.

(7) (a) Mohr, R. R.; Lipscomb, W. N. Structures and energies of diborane(4). *Inorg. Chem.* **1986**, 25, 1053-1057. (b) Knight, L. B. Jr.; Kerr, K.; Miller, P. K.; Arrington, C. A. ESR

Investigation of the HBBH(X3.SIGMA.) Radical in Neon and Argon Matrixes at 4 K. Comparison with ab Initio SCF and CI Calculations. *J. Phys. Chem.* **1995**, *99*, 16842-16848.

(8) Neeve, E. C.; Geier, S. J.; Mkhaliid, I. A. I.; Westcott, S. A.; Marder, T. B. Diboron(4) Compounds: From Structural Curiosity to Synthetic Workhorse. *Chem. Rev.* **2016**, *116*, 9091–9161.

(9) (a) Irvine, G. J.; Lesley, M. J. G.; Marder, T. B.; Norman, N. C.; Rice, C. R.; Robins, E. G.; Roper, W. R.; Whittell, G. R.; Wright, L. J. Transition Metal–Boryl Compounds: Synthesis, Reactivity, and Structure. *Chem. Rev.* **1998**, *98*, 2685–2722. (b) Bontemps, S.; Vendier, L.; Sabo-Etienne, S. Ruthenium-Catalyzed Reduction of Carbon Dioxide to Formaldehyde. *J. Am. Chem. Soc.* **2014**, *136*, 4419–4425.

(10) (a) Ishiyama, T.; Matsuda, N.; Miyaura, N.; Suzuki, A. Platinum(0)-catalyzed diboration of alkynes. *J. Am. Chem. Soc.* **1993**, *115*, 11018-11019. (b) Baker, R. T.; Nguyen, P.; Marder, T. B.; Westcott, S. A. Transition Metal Catalyzed Diboration of Vinylarenes. *Angew. Chem. Int. Ed.* **1995**, *34*, 1336-1338. (c) Mann, G.; John, K. D.; Baker, R. T. Platinum-Catalyzed Diboration Using a Commercially Available Catalyst: Diboration of Aldimines to α -Aminoboronate Esters. *Org. Lett.* **2000**, *2*, 2105-2108. (d) Laitar, D. S.; Müller, P.; Sadighi, J. P. Efficient Homogeneous Catalysis in the Reduction of CO₂ to CO. *J. Am. Chem. Soc.* **2005**, *127*, 17196-17197.

(11) Ishiyama, T.; Miyaura, N. Metal-catalyzed reactions of diborons for synthesis of organoboron compounds. *Chem. Rec.* **2004**, *3*, 271-280.

(12). Ritter, S. K. Boron chemistry branches out. *Chem. Eng. News* **2016**, *94*, 20-23.

- (13) (a) Irvine, G. J.; Lesley, M. J. G.; Marder, T. B.; Norman, N. C.; Rice, C. R.; Robins, E. G.; Roper, W. R.; Whittell, G. R.; Wright, L. J. Transition Metal–Boryl Compounds: Synthesis, Reactivity, and Structure. *Chem. Rev.* **1998**, *98*, 2685 – 2722. (b) Westcott, S. A.; Fernández, E. Singular Metal Activation of Diboron Compounds. *Adv. Organomet. Chem.* **2015**, *63*, 39–89.
- (14) (a) Braunschweig, H.; Wagner, T. Synthesis and Structure of the First Transition Metal Borylene Complexes. *Angew. Chem. Int. Ed.* **1995**, *34*, 825–826. (b) Braunschweig, H.; Colling, M.; Hu, C.; Radacki, K. From Classical to Nonclassical Metal–Boron Bonds: Synthesis of a Novel Metallaborane. *Angew. Chem. Int. Ed.* **2002**, *41*, 1359–1361. (c) Braunschweig, H.; Burschka, C.; Burzler, M.; Metz, S.; Radacki, K. Molecular Structure and Cluster Formation of a tert-Butylborylene Complex. *Angew. Chem. Int. Ed.* **2006**, *45*, 4352–4355.
- (15) (a) Kaesz, H. D.; Fellmann, W.; Wilkes, G. R.; Dahl, L. F. A New Type of Electron-Deficient Compound. A Polyborane Hydridomanganese Carbonyl, $\text{HMn}_3(\text{CO})_{10}(\text{BH}_3)_2$. *J. Am. Chem. Soc.* **1965**, *87*, 2753 – 2755. (b) Arnold, N.; Braunschweig, H.; Dewhurst, R. D.; Ewing, W. C. Unprecedented Borane, Diborane(3), Diborene, and Borylene Ligands via Pt-Mediated Borane Dehydrogenation. *J. Am. Chem. Soc.* **2016**, *138*, 76–79. (c) Sharmila, D.; Mondal, B.; Ramalakshmi, R.; Kundu, S.; Varghese, B.; Ghosh, S. First-Row Transition-Metal–Diborane and –Borylene Complexes. *Chem. Eur. J.* **2015**, *21*, 5074–5083.
- (16) (a) Hata, M.; Kawano, Y.; Shimoi, M. Synthesis and Structure of a Dichromatetraborane Derivative $[\{(\text{OC})_4\text{Cr}\}_2(\eta^4\text{-H,H',H'',H'''}\text{-BH}_2\text{BH}_2\text{-PMe}_2\text{CH}_2\text{PMe}_2)]$. *Inorg. Chem.* **1998**, *37*, 4482–4483. (b) Braunschweig, H.; Damme, A.; Dewhurst, R. D.; Vargas, A. Bond-strengthening π backdonation in a transition-metal π -diborene complex. *Nat. Chem.* **2013**, *5*, 115–121. (c) Wang, S. R.; Prieschl, D.; Mattock, J. D.; Arrowsmith, M.; Prankevicius, C.; Stennett, T. E.;

Dewhurst, R. D.; Vargas, A.; Braunschweig, H. Bottleable Neutral Analogues of $[B_2H_5]^-$ as Versatile and Strongly Binding η^2 Donor Ligands. *Angew. Chem., Int. Ed.* **2018**, *57*, 6347-6351.

(d) Rochette, É.; Bouchard, N.; Lavergne, J. L.; Matta, C. F.; Fontaine, F.-G. Spontaneous Reduction of a Hydroborane To Generate a B–B Single Bond by the Use of a Lewis Pair. *Angew. Chem., Int. Ed.* **2016**, *55*, 12722-12726.

(17) (a) Ting, C.; Messerle, L. Borohydride boron-hydrogen activation and dimerization by a doubly bonded, early-transition-metal organodimetallic complex. Ditantaladiborane syntheses as models for dehydrodimerization of methane to ethane. *J. Am. Chem. Soc.* **1989**, *111*, 3449–3450.

(b) Brunner, H.; Gehart, G.; Meier, W.; Wachter, J.; Wrackmeyer, B.; Nuber, B.; Ziegler, M. L. Präparative, ^{11}B -, ^{93}Nb -NMR-spektroskopische und strukturelle Untersuchungen an Cp_2NbBH_4 - und $[CpNb(B_2H_6)]_2$ -Komplexen. *J. Organomet. Chem.* **1992**, *436*, 313–324. (c) Bose, S. K.; Geetharani, K.; Ramkumar, V.; Mobin, S. M.; Ghosh, S. Fine Tuning of Metallaborane Geometries: Chemistry of Metallaboranes of Early Transition Metals Derived from Metal Halides and Monoborane Reagents. *Chem. Eur. J.* **2009**, *15*, 13483-13490. (d) Anju, R. S.; Roy, D. K.; Mondal, B.; Yuvaraj, K.; Arivazhagan, C.; Saha, K.; Varghese, B.; Ghosh, S. Reactivity of Diruthenium and Dirhodium Analogues of Pentaborane(9): Agostic versus Boratrane Complexes. *Angew. Chem. Int. Ed.*, **2014**, *53*, 2873-2877.

(18) Mondal, B.; Bag, R.; Ghorai, S.; Bakthavachalam, K.; Jemmis, E. D.; Ghosh, S. Synthesis, Structure, Bonding, and Reactivity of Metal Complexes Comprising Diborane(4) and Diborene(2): $[{Cp^*Mo(CO)_2}]_2\{\mu-\eta^2:\eta^2-B_2H_4\}$ and $[{Cp^*M(CO)_2}]_2B_2H_2M(CO)_4$, $M=Mo,W$. *Angew. Chem. Int. Ed.* **2018**, *57*, 8079-8083.

(19) (a) Grebenik, P. D.; Green, M. L. H.; Kelland, M. A.; Leach, J. B.; Mountford, P. Terminal substitution and cage incorporation of an η -cyclopentadienyl ring into borane cage structures; crystal structures of $[\text{Mo}(\eta\text{-C}_5\text{H}_5)(\eta^5\text{:}\eta^1\text{-C}_5\text{H}_4)\text{B}_4\text{H}_7]$ and $[\text{Mo}(\eta\text{-C}_5\text{H}_5)(\eta^3\text{:}\eta^2\text{-C}_3\text{H}_3)\text{C}_2\text{B}_9\text{H}_9]$. *J. Chem. Soc. Chem. Commun.* **1989**, 1397-1399. (b) Saxena, A. K.; Hosmane, N. S. Recent advances in the chemistry of carborane metal complexes incorporating d- and f-block elements. *Chem. Rev.* **1993**, 93, 1081-1124. (c) Fehlner, T. P. Systematic Metallaborane Chemistry. *Organometallics* **2000**, 19, 2643–2651. (d) Kennedy, J. D. The Polyhedral Metallaboranes Part I. Metallaborane Clusters with Seven Vertices and Fewer, Ch. 6. in *Progress in Inorganic Chemistry*, Vol. 32, Lippard, S. J. Ed. **2007**. (e) Kennedy, J. D. The Polyhedral Metallaboranes Part II. Metallaborane Clusters with Eight Vertices and More, Ch. 4, in *Progress in Inorganic Chemistry*, Vol. 34, Lippard, S. J. Ed. **2007**.

(20) (a) De, A.; Zhang, Q.-F.; Mondal, B.; Cheung, L. F.; Kar, S.; Saha, K.; Varghese, B.; Wang, L.-S.; Ghosh, S. $[(\text{Cp}_2\text{M})_2\text{B}_9\text{H}_{11}]$ (M = Zr or Hf): early transition metal ‘guarded’ heptaborane with strong covalent and electrostatic bonding. *Chem. Sci.* **2018**, 9, 1976-1981. (b) Bose, S. K.; Geetharani, K.; Varghese, B.; Mobin, S. M.; Ghosh, S. Metallaboranes of the Early Transition Metals: Direct Synthesis and Characterization of $[\{(\eta^5\text{-C}_5\text{Me}_5)\text{Ta}\}_2\text{B}_n\text{H}_m]$ (n=4, m=10; n=5, m=11), $[\{(\eta^5\text{-C}_5\text{Me}_5)\text{Ta}\}_2\text{B}_5\text{H}_{10}(\text{C}_6\text{H}_4\text{CH}_3)]$, and $[\{(\eta^5\text{-C}_5\text{Me}_5)\text{TaCl}\}_2\text{B}_5\text{H}_{11}]$. *Chem. Eur. J.* **2008**, 14, 9058-9064; (c) Dhayal, R. S.; Chakrahari, K. K. V.; Varghese, B.; Mobin, S. M.; Ghosh, S. Chemistry of Molybdaboranes: Synthesis, Structures, and Characterization of a New Class of Open-Cage Dimolybdaheteroborane Clusters. *Inorg. Chem.* **2010**, 49, 7741-7747. (d) Bose, S. K.; Geetharani, K.; Sahoo, S.; Reddy, K. H. K.; Varghese, B.; Jemmis, E. D.; Ghosh, S. Synthesis, Characterization, and Electronic Structure of New Type of Heterometallic Boride Clusters. *Inorg. Chem.* **2011**, 50, 9414-9422.

- (21) (a) Boron hydride chemistry. Muetterties, E. L. Ed. Academic Press, New York, **1975**.
(b) Fehlner, T. P.; Halet, J.-F.; Saillard, J.-Y.; Molecular Clusters. A Bridge to Solid-State Chemistry, Cambridge University Press: New York, **2007**.
- (22) (a) Housecroft, C. E. Boranes and Metalloboranes: Structure, Bonding and Reactivity. Horwood, E. Chichester; Halsted Press, New York, **1990**. (b) Yan, H.; Beatty, A. M.; Fehlner, T. P. Reactivity of Dimetallapentaboranes—nido-[CpM₂B₃H₇]—with Alkynes: Insertion to Form a Ruthenacarborane (M=RuH) versus Catalytic Cyclotrimerization to Form Arenes (M=Rh). *Angew. Chem. Int. Ed.* **2001**, *40*, 4498-4501. (c) Bose, S. K.; Geetharani, K.; Ghosh, S. C-H activation of arenes and heteroarenes by early transition metallaborane, [(Cp*Ta)₂B₅H₁₁] (Cp* = η^5 -C₅Me₅). *Chem. Commun.* **2011**, *47*, 11996-11998. (d) Geetharani, K.; Tussupbayev, S.; Borowka, J.; Holthausen, M. C.; Ghosh, S. A Mechanistic Study of the Utilization of arachno-Diruthenaborane [(Cp*RuCO)₂B₂H₆] as an Active Alkyne-Cyclotrimerization Catalyst. *Chem. Eur. J.* **2012**, *18*, 8482-8489. (e) Álvarez, Á.; Macías, R.; Bould, J.; Fabra, M. J.; Lahoz, F. J.; Oro, L. A. Alkene Hydrogenation on an 11-Vertex Rhodathiaborane with Full Cluster Participation. *J. Am. Chem. Soc.* **2008**, *130*, 11455-11466.
- (23) (a) Wade, K. The structural significance of the number of skeletal bonding electron-pairs in carboranes, the higher boranes and borane anions, and various transition-metal carbonyl cluster compounds. *J. Chem. Soc. D, Chem. Commun.* **1971**, *0*, 792-793; (b) Wade, K. Structural and Bonding Patterns in Cluster Chemistry. *Adv. Inorg. Chem. Radiochem.* **1976**, *18*, 1-66. (d) Fox, M. A.; Wade, K. Evolving patterns in boron cluster chemistry. *Pure Appl. Chem.* **2003**, *75*, 1315-1323.

- (24) (a) Jemmis, E. D.; Balakrishnarajan, M. M.; Pancharatna, P. D. A Unifying Electron-Counting Rule for Macropolyhedral Boranes, Metallaboranes, and Metallocenes. *J. Am. Chem. Soc.* **2001**, *123*, 4313-4323. (b) Jemmis, E. D.; Balakrishnarajan, M. M.; Pancharatna, P. D. Electronic Requirements for Macropolyhedral Boranes. *Chem. Rev.* **2002**, *102*, 93-144.
- (25) (a) Fehlner, T. P. *Electron Deficient Boron and Carbon Clusters*. Olah, G. A.; Wade, K.; Williams, R. E., Eds. Wiley, New York, **1991**, pp. 287. (b) Kennedy, J. D. *Disobedient Skeletons, The Borane, Carborane, Carbocation Continuum*,. Casanova, J. Ed Wiley, New York, **1998**, pp. 85. (c) Xie, Z. Advances in the chemistry of metallocarboranes of f-block elements. *Coord. Chem. Rev.* **2002**, *231*, 23-46.
- (26) (a) Mondal, B.; Bag, R.; Ghosh, S. Combined Experimental and Theoretical Investigations of Group 6 Dimetallaboranes [(Cp**M*)₂B₄H₁₀] (M = Mo and W). *Organometallics* **2018**, *37*, 2419-2428. (b) Mondal, B.; Bag, R.; Bakthavachalam, K.; Varghese, B. Ghosh, S. Synthesis, Structures, and Characterization of Dimeric Neutral Dithiolato-Bridged Tungsten Complexes. *Eur. J. Inorg. Chem.* **2017**, 5434-5441. (c) Mondal, B.; Bhattacharyya, M.; Varghese, B.; Ghosh, S. Hypo-electronic triple-decker sandwich complexes: synthesis and structural characterization of [(Cp**Mo*)₂{μ-η⁶:η⁶-B₄H₄E-Ru(CO)₃}] (E = S, Se, Te or Ru(CO)₃ and Cp* = η⁵-C₅Me₅). *Dalton Trans.* **2016**, *45*, 10999-11007. (d) Mondal, B.; Mondal, B.; Pal, K.; Varghese, B.; Ghosh, S. An electron-poor di-molybdenum triple-decker with a puckered [B₄Ru₂] bridging ring is an oblate-closo cluster. *Chem. commun.* **2015**, *51*, 3828-3831. (e) Thakur, A.; Chakrahari, K. K. V.; Mondal, B.; Ghosh, S. Novel Triple-Decker Sandwich Complex with a Six-Membered [B₃Co₂(μ₄-Te)] Ring as the Middle Deck. *Inorg. Chem.* **2013**, *52*, 2262-2264. (f) Sahoo, S.; Reddy, K. H. K.; Dhayal, R. S.; Mobin, S. M.; Ramkumar, V.; Jemmis, E. D.; Ghosh, S. Chlorinated Hypoelectronic Dimetallaborane Clusters: Synthesis,

Characterization, and Electronic Structures of $(\eta^5\text{-C}_5\text{Me}_5\text{W})_2\text{B}_5\text{H}_n\text{Cl}_m$ ($n = 7, m = 2$ and $n = 8, m = 1$). *Inorg. Chem.* **2009**, *48*, 6509-6516.

(27) Aldridge, S.; Shang, M.; Fehlner, T. P. Synthesis of Novel Molybdaboranes from $(\eta^5\text{-C}_5\text{R}_5)\text{MoCl}_n$ Precursors ($\text{R} = \text{H, Me; } n = 1, 2, 4$). *J. Am. Chem. Soc.* **1998**, *120*, 2586-2598.

(28) Dhayal, R. S.; Sahoo, S.; Reddy, K. H. K.; Mobin, S. M.; Jemmis, E. D.; Ghosh, S. Vertex-Fused Metallaborane Clusters: Synthesis, Characterization and Electronic Structure of $[(\eta^5\text{-C}_5\text{Me}_5\text{Mo})_3\text{MoB}_9\text{H}_{18}]$. *Inorg. Chem.* **2010**, *49*, 900-904.

(29) (a) Snow, S. A.; Shimoi, M.; Ostler, C. D.; Thompson, B. K.; Kodama, G.; Parry, R. W. Metal complexes of the neutral borane adduct $(\text{B}_2\text{H}_4 \cdot 2\text{P}(\text{CH}_3)_3)$. *Inorg. Chem.* **1984**, *23*, 511-512.

(b) Katoh, K.; Shimoi, M.; Ogino, H. Syntheses and structures of $[\text{M}(\text{CO})_5\{\text{B}_2\text{H}_4 \cdot 2\text{P}(\text{CH}_3)_3\}]$ and $[\text{M}(\text{CO})_4\{\text{B}_2\text{H}_4 \cdot 2\text{P}(\text{CH}_3)_3\}]$ ($\text{M} = \text{chromium, molybdenum, tungsten}$). *Inorg. Chem.* **1992**, *31*, 670-675.

(30) (a) Bailey, W. I. Jr.; Chisholm, M. H.; Cotton, F. A.; Rankel, L. A. Reactions of metal-to-metal multiple bonds. 4. μ -Acetylene-bis(cyclopentadienyl)tetracarbonyldimolybdenum compounds. Preparations, properties, structural characterizations, and dynamical solution behavior. *J. Am. Chem. Soc.* **1978**, *100*, 5764-5773. (b) Fleischmann, M.; Jones, J. S.; Balázs, G.; Gabbai, F. P.; Scheer, M. Supramolecular adducts based on weak interactions between the trimeric Lewis acid complex (perfluoro-*ortho*-phenylene)mercury and polypnictogen complexes. *Dalton Trans.* **2016**, *45*, 13742-13749.

(31) Jun, C.-S.; Halet, J.-F.; Rheingold, A. L.; Fehlner, T. P. Preparation and Characterization of Cobaltaboranes Containing Cobalt Carbonyl Fragments. *Inorg. Chem.* **1995**, *34*, 2101-2107.

- (32) Total skeletal electron pair (sep) of **2** is 6 and total valence electron (tve) is 40.
- (33) (a) Mingos, D. M. P. A General Theory for Cluster and Ring Compounds of the Main Group and Transition Elements. *Nat. Phys. Sci.* **1972**, 236, 99–102. (b) Welch, A. J. The significance and impact of Wade's rules. *Chem. Commun.* **2013**, 49, 3615–3616.
- (34) Aldridge, S.; Fehlner, T. P.; Shang, M. Directed Synthesis of Chromium and Molybdenum Metallaborane Clusters. Preparation and Characterization of (Cp*Cr)₂B₅H₉, (Cp*Mo)₂B₅H₉, and (Cp*MoCl)₂B₄H₁₀. *J. Am. Chem. Soc.* **1997**, 119, 2339–2340.
- (35) Weller, A. S.; Shang, M.; Fehlner, T. P. Synthesis of Mono- and Ditungstaboranes from Reaction of Cp*WCl₄ and [Cp*WCl₂]₂ with BH₃·thf or LiBH₄ (Cp* = η⁵-C₅Me₅). Control of Reaction Pathway by Choice of Monoboron Reagent and Oxidation State of Metal Center. *Organometallics* **1999**, 18, 53–64.
- (36) Computed ¹¹B NMR chemical shifts (for **3'** and **5'**, the Cp analogues of **3** and **4**) employing GIAO method satisfactorily helped us to assign all the boron atoms with a margin of error ~10 ppm, whereas, for **5'** (the Cp analogue of **5**) ca. 40 ppm error was observed (see Table S1).
- (37) Lei, X.; Shang, M.; Fehlner, T. P. 2,2'-commo-Bis[2-ruthena-nido-1-(η⁵-pentamethylcyclopentadienyl)ruthenahexaborane(12)]: An Unusual Ruthenaborane Related to Ruthenocene and Exhibiting a Linear Triruthenium Fragment. *Angew. Chem. Int. Ed.* **1999**, 38, 1986–1989.
- (38) (a) Corbett, J. D. Extended metal-metal bonding in halides of the early transition metals. *Acc. Chem. Res.* **1981**, 14, 239–246. (b) Kennedy, J. D. The Polyhedral Metallaboranes Part I. Metallaborane Clusters with Seven Vertices and Fewer. *Prog. Inorg. Chem.* **1984**, 32, 519–679.

(c) Kennedy, J. D. The Polyhedral Metallaboranes Part II. Metallaborane Clusters with Eight Vertices and More. *Prog. Inorg. Chem.* **1986**, *34*, 211-434. (d) Ghosh, S.; Fehlner, T. P.; Noll, B. C. Condensed metallaborane clusters: synthesis and structure of $\text{Fe}_2(\text{CO})_6(\eta^5\text{-C}_5\text{Me}_5\text{RuCO})(\eta^5\text{-C}_5\text{Me}_5\text{Ru})\text{B}_6\text{H}_{10}$. *Chem. Commun.* **2005**, 3080-3082. (e) Wong, K.-S.; Bowser, J. R.; Pipal, J. R.; Grimes, R. N. Tetracarbon metallocarboranes. 5. A new synthetic route: synthesis of $\text{Co}_2\text{C}_4\text{B}_6$ and CoC_4B_7 nido cage systems by fusion of dicarbon cobaltacarboranes in ethanolic potassium hydroxide. Crystal structure of $(\eta^5\text{-C}_5\text{H}_5)_2\text{Co}_2\text{C}_4\text{B}_6\text{H}_{10}$. *J. Am. Chem. Soc.* **1978**, *100*, 5045-5051. (f) Mingos, D. M. P. Polyhedral skeletal electron pair approach. *Acc. Chem. Res.* **1984**, *17*, 311-319. (g) Grimes, R. N. Cluster forming and cage fusion in metallocarborane chemistry. *Coord. Chem. Rev.* **1995**, *143*, 71-96. (h) Kennedy, J. D. In *Advances in Boron Chemistry*; Siebert, W., Ed.; Royal Society of Chemistry: Cambridge, U. K., **1997**, pp 451.

(39) This can be explained qualitatively as; W3 is in bonding contact with W1, W2, B4 and two hydride ligands that contributes total of 5 electrons which is equal to that of a $\eta^5\text{-Cp}$ or Cp^* ligand. Molecular orbital calculation together with NBO analysis further supports the same.

(40) (a) Wang, Y.; Quillian, B.; Wei, P.; Wannere, C. S.; Xie, Y.; King, R. B.; Schaefer, H. F. III; Schleyer, P. v. R.; Robinson, G. H. A Stable Neutral Diborene Containing a B=B Double Bond. *J. Am. Chem. Soc.* **2007**, *129*, 12412-12413. (b) Scheschkewitz, D. A Base-Stabilized Neutral B=B Bond: Closing a Gap by Filling the Void. *Angew. Chem. Int. Ed.* **2008**, *47*, 1995-1997. (c) Wang, Y.; Quillian, B.; Wei, P.; Xie, Y.; Wannere, C. S.; King, R. B.; Schaefer, H. F. III; Schleyer, P. v. R.; Robinson, G. H. Planar, Twisted, and Trans-Bent: Conformational Flexibility of Neutral Diborenes. *J. Am. Chem. Soc.* **2008**, *130*, 3298-3299. (d) Wang, Y.; Robinson, G. H. Carbene Stabilization of Highly Reactive Main-Group Molecules. *Inorg. Chem.*

2011, *50*, 12326–12337. (e) Wang, Y.; Robinson, G. H. N-Heterocyclic Carbene—Main-Group Chemistry: A Rapidly Evolving Field. *Inorg. Chem.* **2014**, *53*, 11815–11832.

(41) (a) Mitoraj, M. P.; Michalak, A. Multiple Boron–Boron Bonds in Neutral Molecules: An Insight from the Extended Transition State Method and the Natural Orbitals for Chemical Valence Scheme. *Inorg. Chem.* **2011**, *50*, 2168–2174. (b) Braunschweig, H.; Dewhurst, R. D. Single, Double, Triple Bonds and Chains: The Formation of Electron-Precise B–B Bonds. *Angew. Chem. Int. Ed.* **2013**, *52*, 3574–3583. (c) Braunschweig, H.; Dewhurst, R. D. Boron–Boron Multiple Bonding: From Charged to Neutral and Back Again. *Organometallics* **2014**, *33*, 6271–6277. (d) Brand, J.; Braunschweig, H.; Sen, S. S. B=B and B=E (E = N and O) Multiple Bonds in the Coordination Sphere of Late Transition Metals. *Acc. Chem. Res.* **2014**, *47*, 180–191. (e) Fischer, R. C.; Power, P. P. π -Bonding and the Lone Pair Effect in Multiple Bonds Involving Heavier Main Group Elements: Developments in the New Millennium. *Chem. Rev.* **2010**, *110*, 3877–3923. (f) Power, P. P. Interaction of Multiple Bonded and Unsaturated Heavier Main Group Compounds with Hydrogen, Ammonia, Olefins, and Related Molecules. *Acc. Chem. Res.* **2011**, *44*, 627–637.

(42) (a) Hashimoto, H.; Shang, M.; Fehlner, T. P. Clusters as Ligands. Coordination of an Electronically Unsaturated Chromaborane to an Iron Tricarbonyl Fragment. *J. Am. Chem. Soc.* **1996**, *118*, 8164–8165. (b) Aldridge, S.; Hashimoto, H.; Kawamura, K.; Shang, M.; Fehlner, T. P. Cluster Expansion Reactions of Group 6 Metallaboranes. Syntheses, Crystal Structures, and Spectroscopic Characterizations of $(\text{Cp}^*\text{Cr})_2\text{B}_5\text{H}_9$, $(\text{Cp}^*\text{Cr})_2\text{B}_4\text{H}_8\text{Fe}(\text{CO})_3$, $(\text{Cp}^*\text{Cr})_2\text{B}_4\text{H}_7\text{Co}(\text{CO})_3$, and $(\text{Cp}^*\text{Mo})_2\text{B}_5\text{H}_9\text{Fe}(\text{CO})_3$. *Inorg. Chem.* **1998**, *37*, 928–940.

(43) The asymmetric unit of **7** contains four independent molecules which differ little in terms of geometric parameters. As a result, the structural data presented in Figure 6 (a) is from one of the units.

(44) (a) Handy, L. B.; Ruff, J. K.; Dahl, L. F. Structural characterization of the dinuclear metal carbonyl anions $[M_2(CO)_{10}]^{2-}$ (M = chromium, molybdenum) and $[Cr_2(CO)_{10}H]^-$. Marked stereochemical effect of a linearly protonated metal-metal bond. *J. Am. Chem. Soc.* **1970**, 92, 7312-7326. (b) Scherer, O. J.; Sitzmann, H.; Wolmershäuser, G. Umsetzung von P_4 mit $(\eta^5-C_5H_5)(CO)_2Mo\equiv Mo(CO)_2(\eta^5-C_5H_5)$ zu den tetraedrischen molybdänkomplexen $P_n[Mo(CO)_2(\eta^5-C_5H_5)]_{4-n}$ ($n = 2, 3$). *J. Organomet. Chem.* **1984**, 268, C9-C12.

(45) (a) Dahyal, R. S.; Sahoo, S.; Ramkumar, V.; Ghosh, S. Substitution at boron in molybdaborane frameworks: Synthesis and characterization of isomeric $(\eta^5-C_5Me_5Mo)_2B_5H_nX_m$ (when $X=Cl$: $n=5, 7, 8$; $m=4, 2, 1$ and $X=Me$: $n=6, 7$; $m=3, 2$). *J. Organomet. Chem.* **2009**, 694, 237–243. (b) Green, M. L. H.; Hubert, J. D.; Mountford, P. Synthesis of the $W\equiv W$ triply bonded dimers $[W_2(\eta^5-C_5H_4R)_2X_4]$ ($X = Cl$, $R = Me$ or Pri ; $X = Br$, $R = Pri$) and X-ray crystal structures of $[W(\eta^5-C_5H_4Pri)Cl_4]$ and $[W_2(\eta-C_5H_4Pri)_2Cl_4]$. *J. Chem. Soc. Dalton Trans.* **1990**, 3793–3800. (c) Kaushika, M.; Singh, A.; Kumar, M. The chemistry of group-VIb metal carbonyls. *Eur. J. Chem.* **2012**, 3, 367–394.

(46) Ryschkewitsch, G. E.; Nainan, K. C. Octahydrotriborate(1-) $[B_3H_8]$ salt. *Inorg. Synth.* **1974**, 15, 113–114.

(47) Gaussian 09, Frisch, M. J. et al., Gaussian, Inc., Wallingford CT, **2010** (for detailed reference see supporting information).

- (48) (a) Schmider, H. L.; Becke, A. D. Optimized density functionals from the extended G2 test set. *J. Chem. Phys.* **1998**, *108*, 9624-9631. (b) Perdew, J. P. Density-functional approximation for the correlation energy of the inhomogeneous electron gas. *Phys. Rev. B* **1986**, *33*, 8822-8824.
- (49) Weigend, F.; Ahlrichs, R. Balanced basis sets of split valence, triple zeta valence and quadruple zeta valence quality for H to Rn: Design and assessment of accuracy. *Phys. Chem. Chem. Phys.* **2005**, *7*, 3297-3305.
- (50) Andrae, D.; Häußermann, U.; Dolg, M.; Stoll, H.; Preuss, H. Energy-adjusted ab initio pseudopotentials for the second and third row transition elements. *Theor. Chim. Acta.* **1990**, *77*, 123-141.
- (51) (a) Becke, A. D. Density-functional exchange-energy approximation with correct asymptotic behavior. *Phys. Rev. A* **1988**, *38*, 3098-3100. (b) Lee, C.; Yang, W.; Parr, R. G. Development of the Colle-Salvetti correlation-energy formula into a functional of the electron density. *Phys. Rev. B* **1988**, *37*, 785-789. (c) Becke, A. D. Density-functional thermochemistry. III. The role of exact exchange. *J. Chem. Phys.* **1993**, *98*, 5648-5651.
- (52) (a) London, F. Théorie quantique des courants interatomiques dans les combinaisons aromatiques. *J. Phys. Radium.* **1937**, *8*, 397-409. (b) Ditchfield, R. Self-consistent perturbation theory of diamagnetism. *Mol. Phys.* **1974**, *27*, 789-807. (c) Wolinski, K.; Hinton, J. F.; Pulay, P. Efficient implementation of the gauge-independent atomic orbital method for NMR chemical shift calculations. *J. Am. Chem. Soc.* **1990**, *112*, 8251-8260.
- (53) (a) Glendening, E. D.; Reed, A. E.; Carpenter, J. E.; Weinhold, F. *NBO Program 3.1*, W. T. Madison: 1988; (b) Reed, A. E.; Weinhold, F.; Curtiss, L. A. Intermolecular interactions from

a natural bond orbital, donor-acceptor viewpoint. *Chem. Rev.* **1988**, 88, 899–926. (c) Weinhold, F.; Landis, R. *Valency and bonding: A natural bond orbital donor-acceptor perspective*. Cambridge University Press: Cambridge; U.K, 2005.

(54) Wiberg, K. B. Application of the pople-santry-segal CNDO method to the cyclopropylcarbiny and cyclobutyl cation and to bicyclobutane. *Tetrahedron* **1968**, 24, 1083–1096.

(55) (a) Bader, R. F. W. *Atoms in Molecules: a Quantum Theory*; Oxford University Press: Oxford, U. K. 1990. (b) Bader, R. F. W. A Bond Path: A Universal Indicator of Bonded Interactions. *J. Phys. Chem. A.* **1998**, 102, 7314–7323. (c) Bader, R. F. W. A quantum theory of molecular structure and its applications. *Chem. Rev.* **1991**, 91, 893–928.

(56) Lu, T.; Chen, F. Multiwfn: A multifunctional wavefunction analyzer. *J. Comput. Chem.* **2012**, 33, 580–592.

(57) Bruker (2004). APEX2, SAINT and SADABS. Bruker AXS Inc., Madison, Wisconsin, USA.

(58) Sheldrick, G. M. SHELXS-97; University of Göttingen (Germany), **1997**.

(59) Sheldrick, G. M. Crystal structure refinement with SHELXL. *Acta Cryst.* **2015**, C71, 3–8.

For Table of Contents Only

Use of Single Metal Fragments for Cluster Building: Synthesis, Structure and Bonding of Heterometallaboranes

Using CO gas we have synthesized an extremely fluxional molybdenum diborane(4) species, $[\{\text{Cp}^*\text{Mo}(\text{CO})_2\}_2\{\mu\text{-}\eta^2\text{:}\eta^2\text{-B}_2\text{H}_4\}]$ that mimic Cotton's dimolybdenum-acetylene complex, $[\{\text{CpMo}(\text{CO})_2\}_2\text{C}_2\text{H}_2]$. In addition, we have isolated and structurally characterized a homoleptic molybdaborane, $[(\text{Cp}^*\text{Mo})_3(\mu\text{-H})_2(\mu_3\text{-H})(\mu\text{-CO})_2\text{B}_4\text{H}_4]$, and a vertex-fused cluster, $[(\text{Cp}^*\text{W})_3\text{WB}_9\text{H}_{18}]$ (see picture).

